The Harry Emmett Gunning Lecture Series
October 2-4, 2002
Department of Chemistry
The University of Alberta
Edmonton, Alberta

Lecture 1

The nucleus as a reporter, the NMR chemical shift

Cynthia J. Jameson
University of Illinois at Chicago

$W = -\mu \bullet \mathbf{B}_0$ bare nucleus $\quad \mu = \gamma \hbar \mathbf{I}$

For spin I = ½ with magnetogyric ratio γ, resonance frequency $\omega = \gamma B_0$

W. G. Proctor and F. C. Yu
Phys. Rev. **1951**, 81, 20.
Measure μ based on accurately known magnetic moment of the proton:

	relative frequency
$K_3Co(CN)_6$	1.0000
$Co(C_2H_4(NH_2)_3Cl_3$	1.0073 ± 0.0001
$Na_3Co(NO_2)_6$	1.0074 ± 0.0001
$Co(NH_3)_6Cl_3$	1.0083 ± 0.0001
$K_3Co(C_2O_4)_3$	1.0130 ± 0.0001

1.3% ***site specific!***

$W = -\mu \bullet (\mathbf{u_B} - \sigma \bullet \mathbf{u_B}) B_0$

$\omega = |\gamma| B_0 [\mathbf{u_B}^{\dagger} \bullet (\mathbf{1}-\sigma^{\dagger})(\mathbf{1}-\sigma) \bullet \mathbf{u_B}]^{1/2}$

The observed chemical shift

- **The shielding surface:** the intrinsic shielding response at the position of the nucleus
- **Averaging**

When we observe a chemical shift in NMR, the nucleus reports on both.

In all cases, the observed average comes from the shielding value at each point on the shielding surface being weighted according to the probability of finding the molecular system at that nuclear configuration.

The intrinsic shielding response depends on the atom at the position of the nucleus

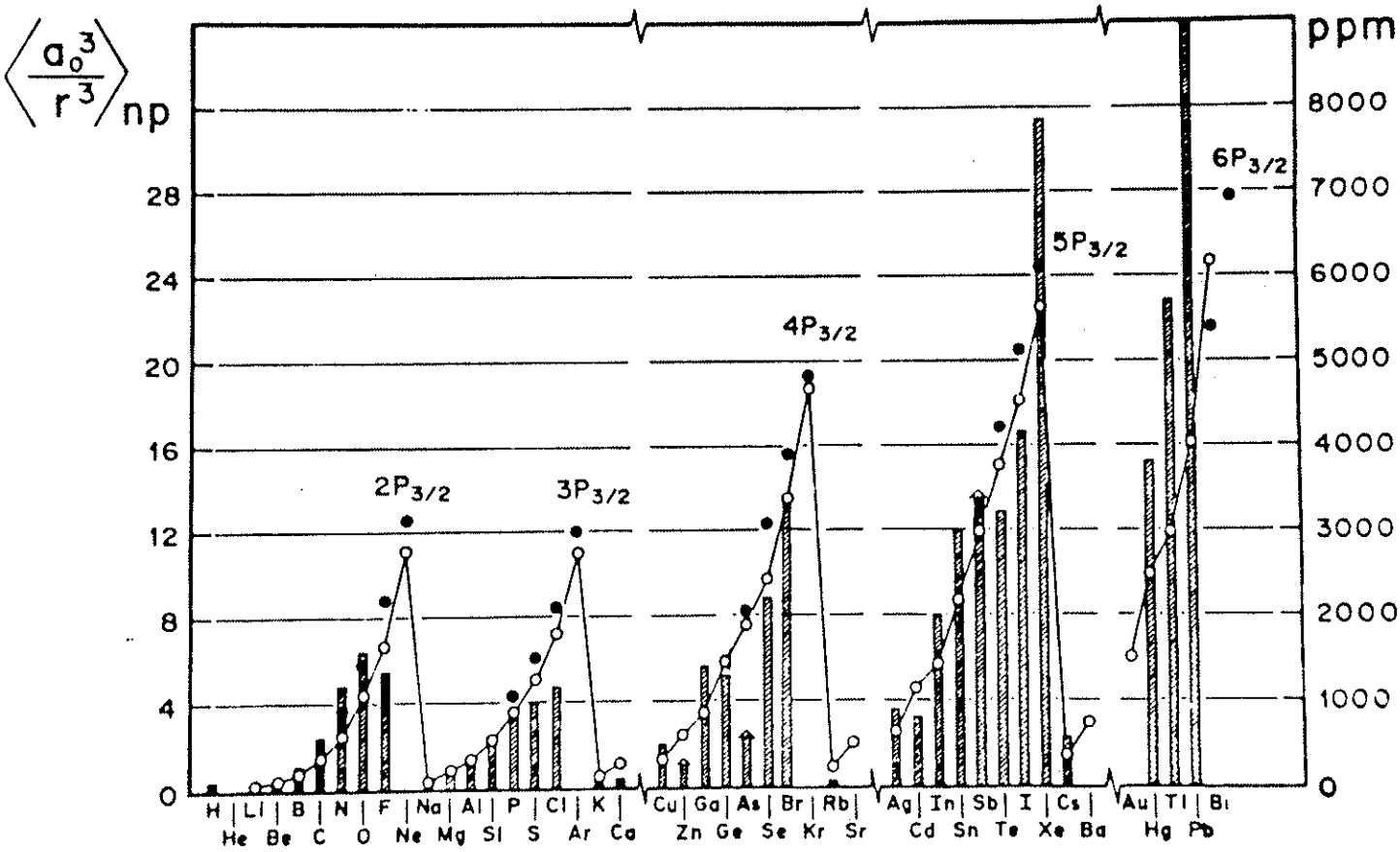

In the Ramsey formulae, the operators that lead to the NMR chemical shift involve $\sum_i L_{z,i}$ and $\sum_i L_{z,i}/r_i^3$.

"An experimental quantity which gives a quite direct measure of $\langle 1/r^3 \rangle$ is the spin orbit interaction, which is available from tables of atomic energy levels."

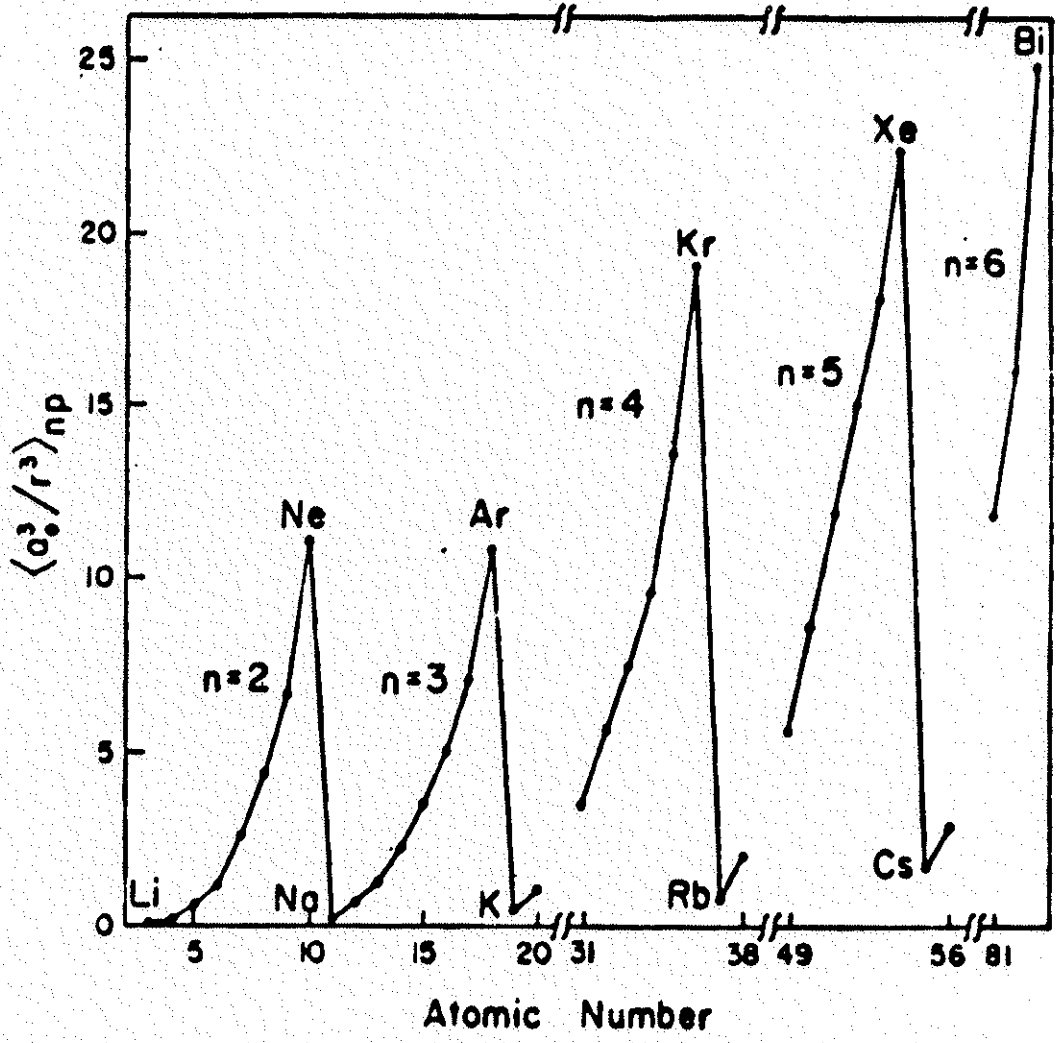

FIG. 1. The variation of $\langle a_0^3/r^3 \rangle_{np}$ with atomic number, as calculated, mainly in Ref. 15, from the observed atomic spin-orbit splittings without relativistic correction.

Shielding surfaces

intramolecular

bond length
bond angle
torsion angle

OBSERVATIONS

- mass dependence → isotope shifts

- temperature dependence at the zero-density limit

- structure!

The shielding surface

The nuclear magnetic shielding as a function of nuclear coordinates of a molecule, (distances, bond angles,..)

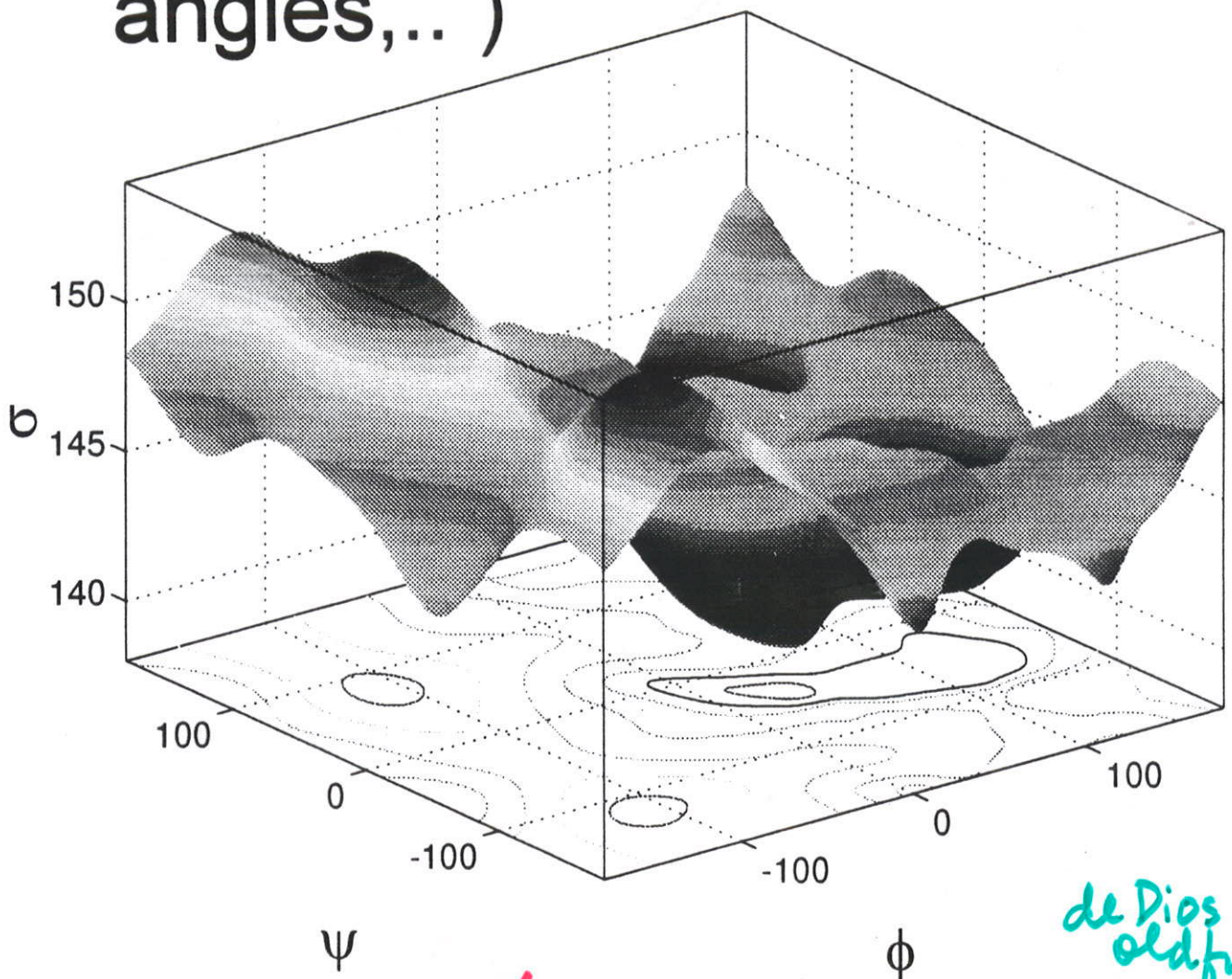

de Dios and Oldfield

C^{α} in alanine

Shielding surfaces and averaging

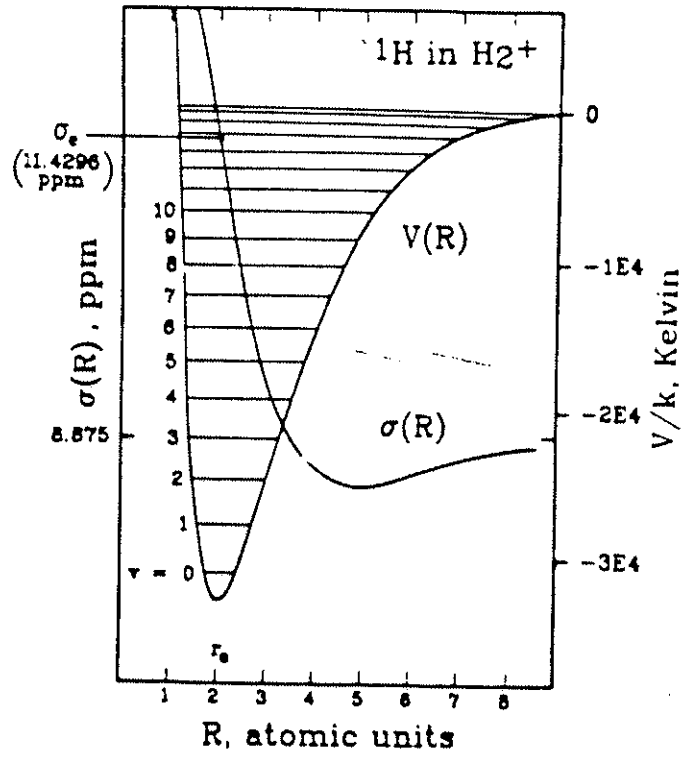

The ^{1}H shielding surface: In the vicinity of the equilibrium geometry, the proton becomes less shielded with increasing bond length

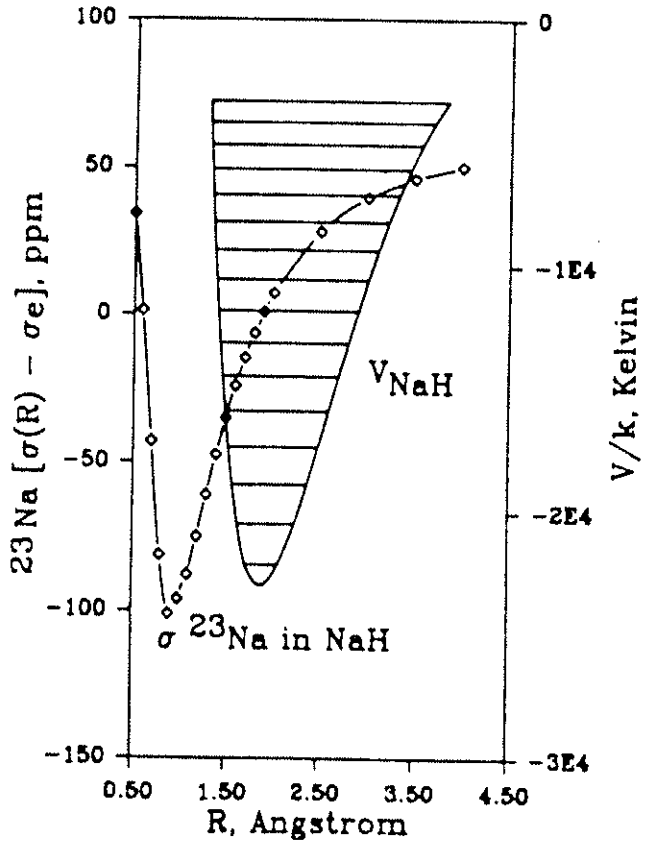

The ^{23}Na becomes more shielded with increasing bond length

The probability of finding a molecule at a given nuclear configuration is given by $|\Psi_{vib}|^2$.

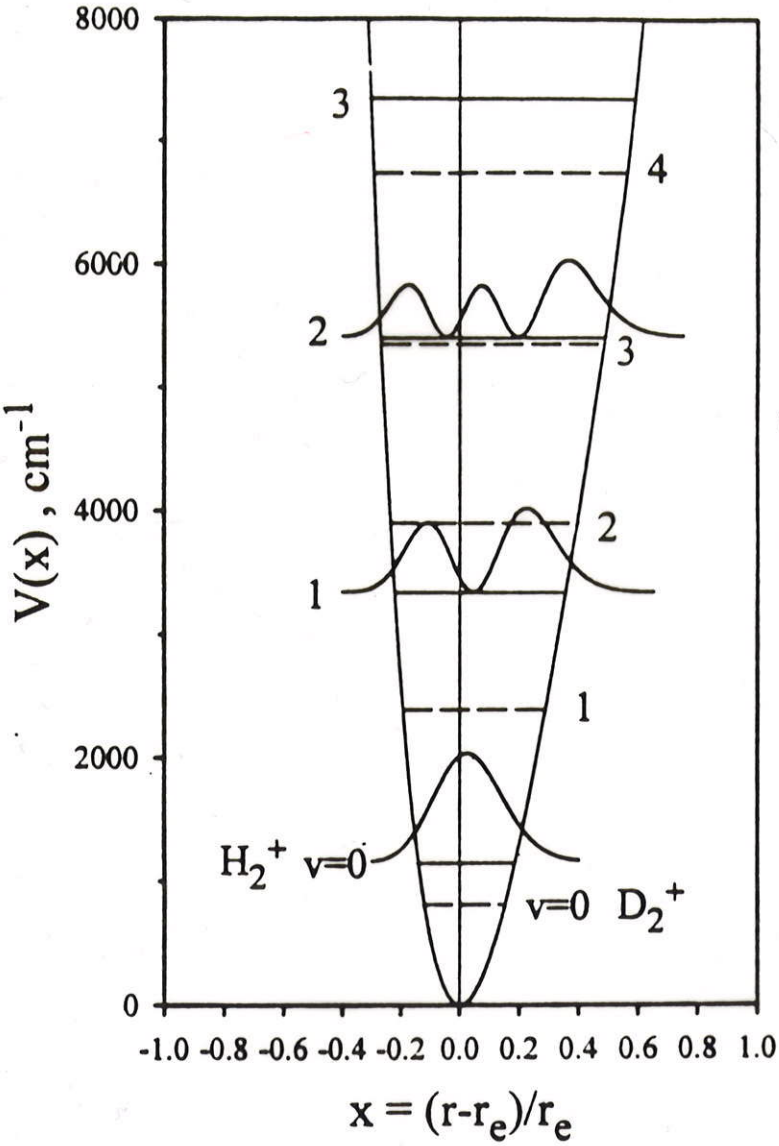

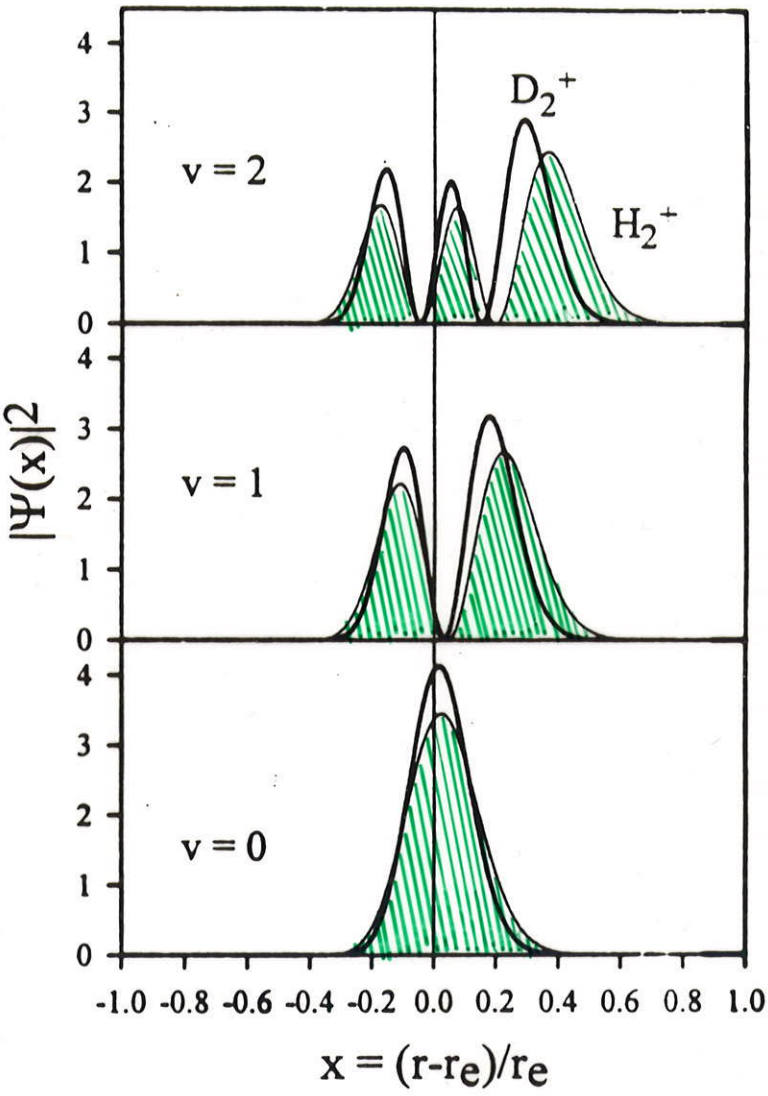

This is mass-dependent.

Dynamic averages

To get the average value of a molecular electronic property:

$$\langle P \rangle_v = \int_{-\infty}^{+\infty} |\Psi_v(x)|^2 P(x) dx$$

We can also find the rotational average. The thermal average is

$$\langle P \rangle^T = \frac{\sum_{v,J,K} (2J+1) g_{Ns} \langle P \rangle_{vJK} \exp(-E_{vJK}/kT)}{\sum_{v,J,K} (2J+1) g_{Ns} \exp(-E_{vJK}/kT)}$$

We can see that the low frequency vibrations are important, but also those vibrational modes that have large $\langle P \rangle_{vJ}$

TEMPERATURE DEPENDENCE IN THE ZERO-PRESSURE LIMIT

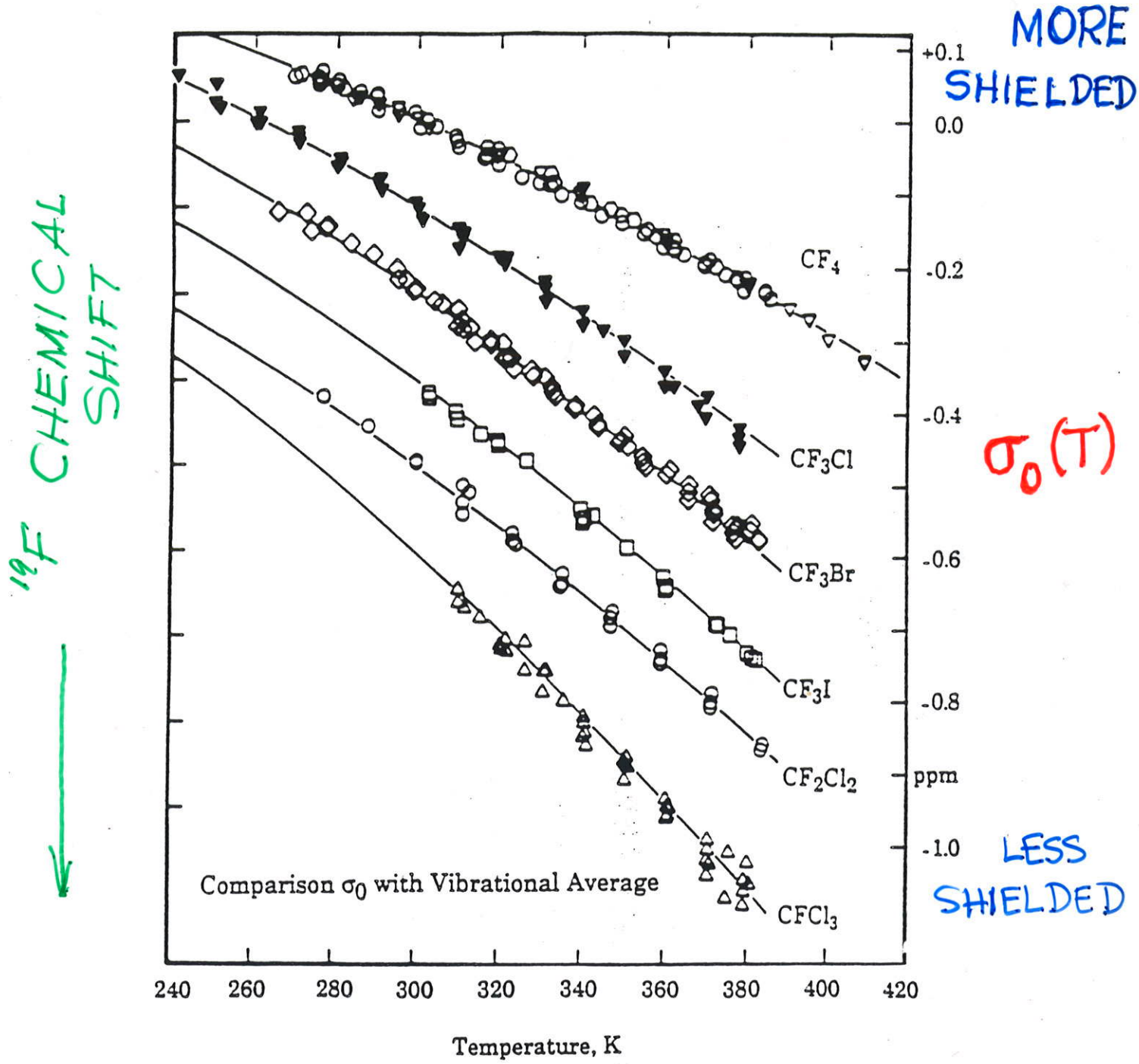

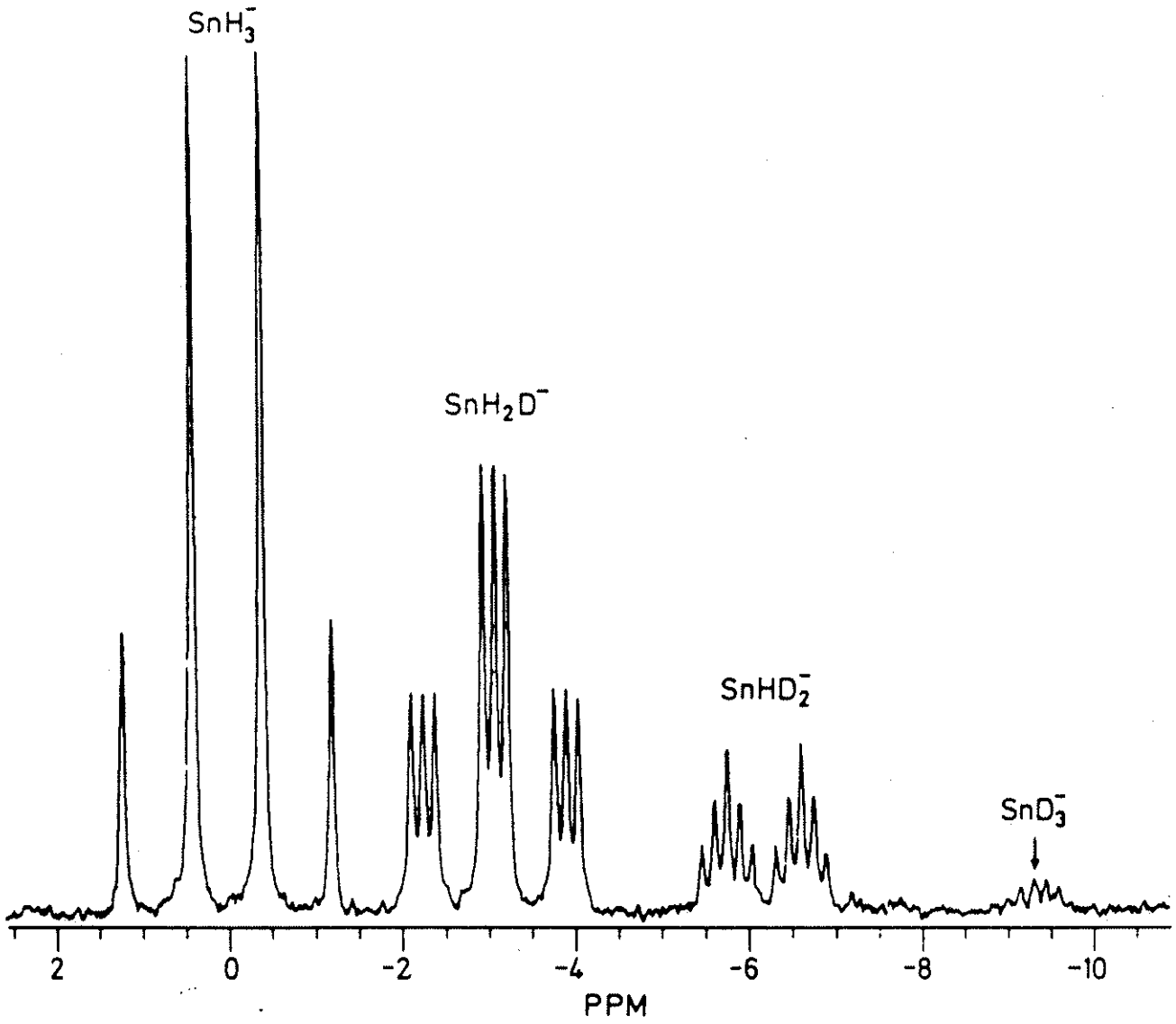

^{119}Sn D-induced isotope shifts in the deuterated SnH_3^- species are -3.281 ppm / D

Wasylishen and Burford

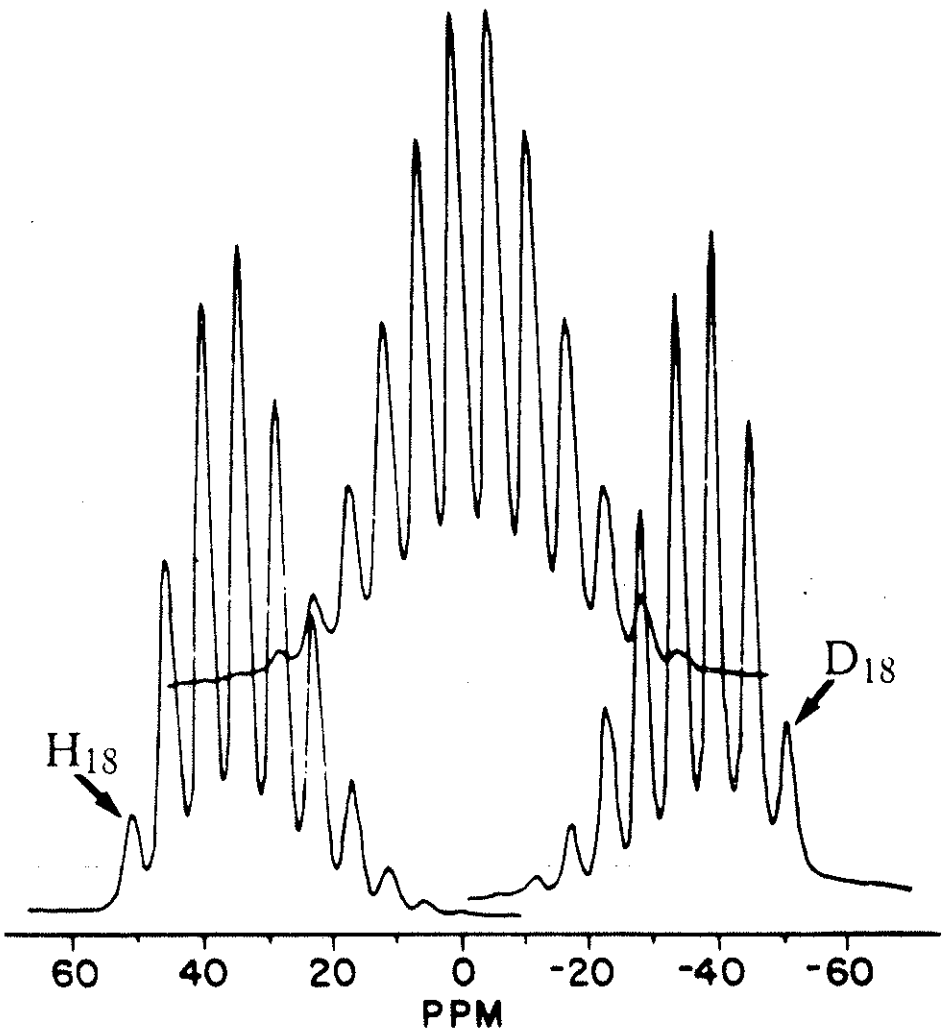

^{59}Co NMR spectrum of 3 samples of deuterated $^{59}Co[(NH_3)_6]^{2+}$

$$I = \frac{18!}{p!(18-p)!}(1-d)^p(d)^{(18-p)}$$

d = overall deuterium fraction in sample

$d = 0.15, 0.50, 0.85$ from left to right

Russell and Bryant

SUMMARY

- Where an isotopic label is introduced in a molecule, every neighboring NMR nucleus experiences a slight chemical shift.
- If labeling is less than 100%, the resonant nuclei in both the labeled and the unlabeled molecules are observed, with intensities according to statistical distribution.
- The magnitude of the shift depends on the fractional mass change at the isotope substitution site, on the remoteness of the resonant nucleus from the substitution site, and on the sensitivity of the chemical shift of the resonant nucleus; the latter is reflected by the chemical shift range of that nucleus.

- The isotope shift is just one more powerful tool in which a very selective tag carries with it the same wealth of information as the chemical shift itself.
- Isotope shifts provide a more stringent test of ab initio calculations of chemical shifts in specific molecules, being directly related to the slopes on the mathematical surface that describes the variation of the chemical shift with the molecular geometry.
- In a more general sense, the trends in the thousands of isotope shifts that have been accumulated provide insight into the general nature of these chemical shift surfaces, in terms of the dependence of the details of the surface on the nature of the chemical bond, the net charge of the molecule, bond orders, presence of lone pairs, etc.

The folding of a protein into its native conformation causes NMR chemical shift nonequivalencies to be introduced.

Spera and Bax (1991): helical and sheet segments could be clearly differentiated based on their C^{α} and C^{β} chemical shifts. Therefore, ^{13}C chemical shifts in proteins are sensitive to backbone ϕ and Ψ torsion angles.

A. C. de Dios, E. Oldfield and coworkers calculated shielding surfaces (*Science* 1993), reproduced Spera and Bax

^{13}C and ^{15}N nuclei in amino acid residues in peptides and proteins report on local geometric or electronic structure, in particular the backbone and sidechain torsion angles.

Alanine Shielding Surface

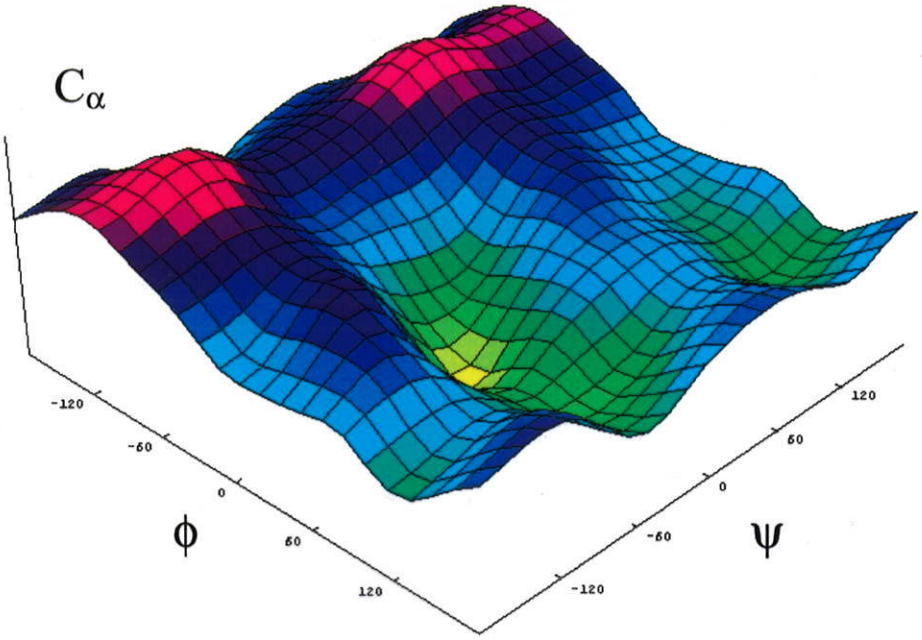

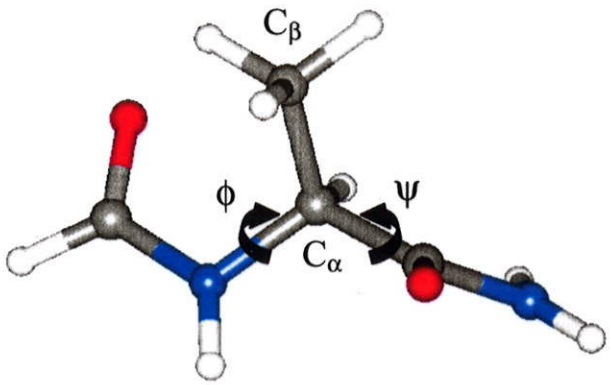

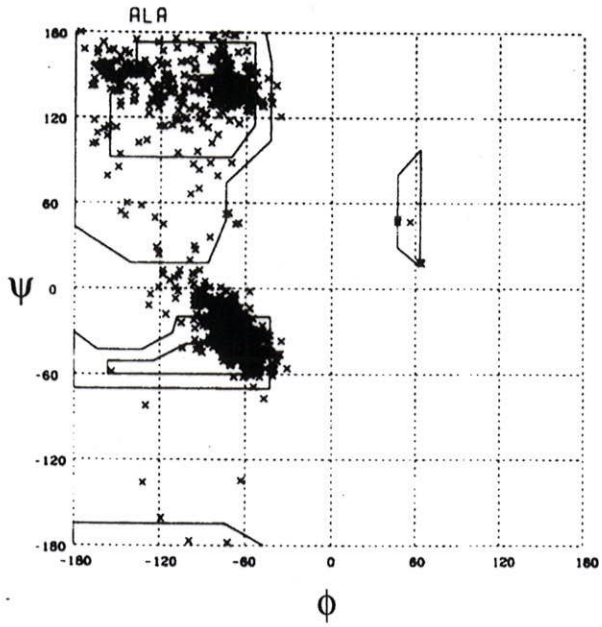

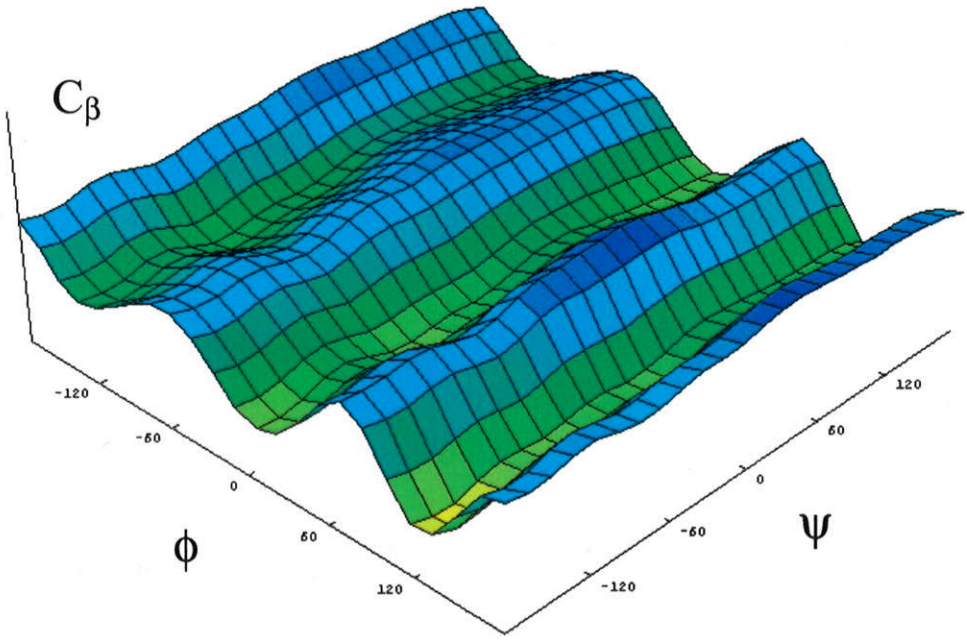

de Dios AC, Pearson JG, Oldfield E. Science. 260, 1491-1496. **1993**.

Characterization of Polymorphous Verbanol[6]

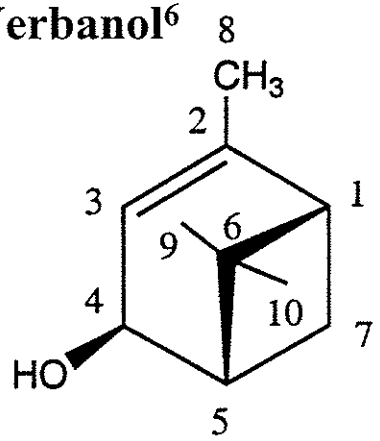

→ Major polymorphic form with known x-ray structure and a minor form with unknown structure

→ NMR experiments

⇒ CPMAS and 2D FIREMAT

→ QM CST calculations

⇒ peak assignments

→ Spectral results

⇒ CST for each carbon site could be extracted

⇒ Spectra clearly indicate 3 and 4 distinct molecules per asymmetric unit for major and minor forms, respectively

→ Fairly rigid structure

⇒ Variation in structure is associated with C3-C4-O-H dihedral angle

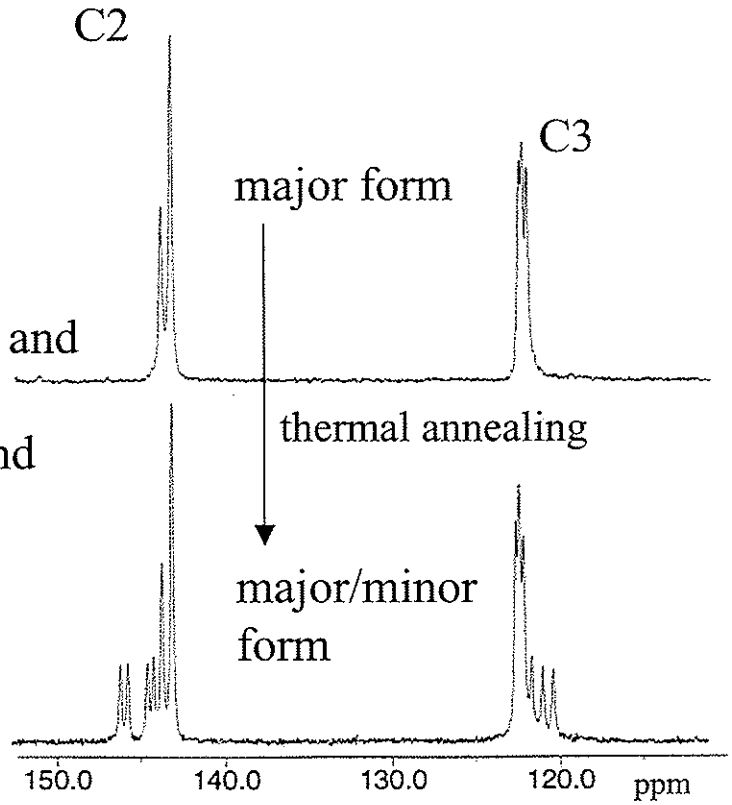

[6] J. K. Harper and D. M. Grant; *J. Am. Chem. Soc.*, **122**, 3708 (2000)

Shielding surfaces
intermolecular

OBSERVATIONS:
dependence on:

- phase, density
- number of neighbors
- electronic structure of neighbors
- 'ring currents'
- chirality
- size, shape of confining structure
- coverage
- nuclear site in the molecule

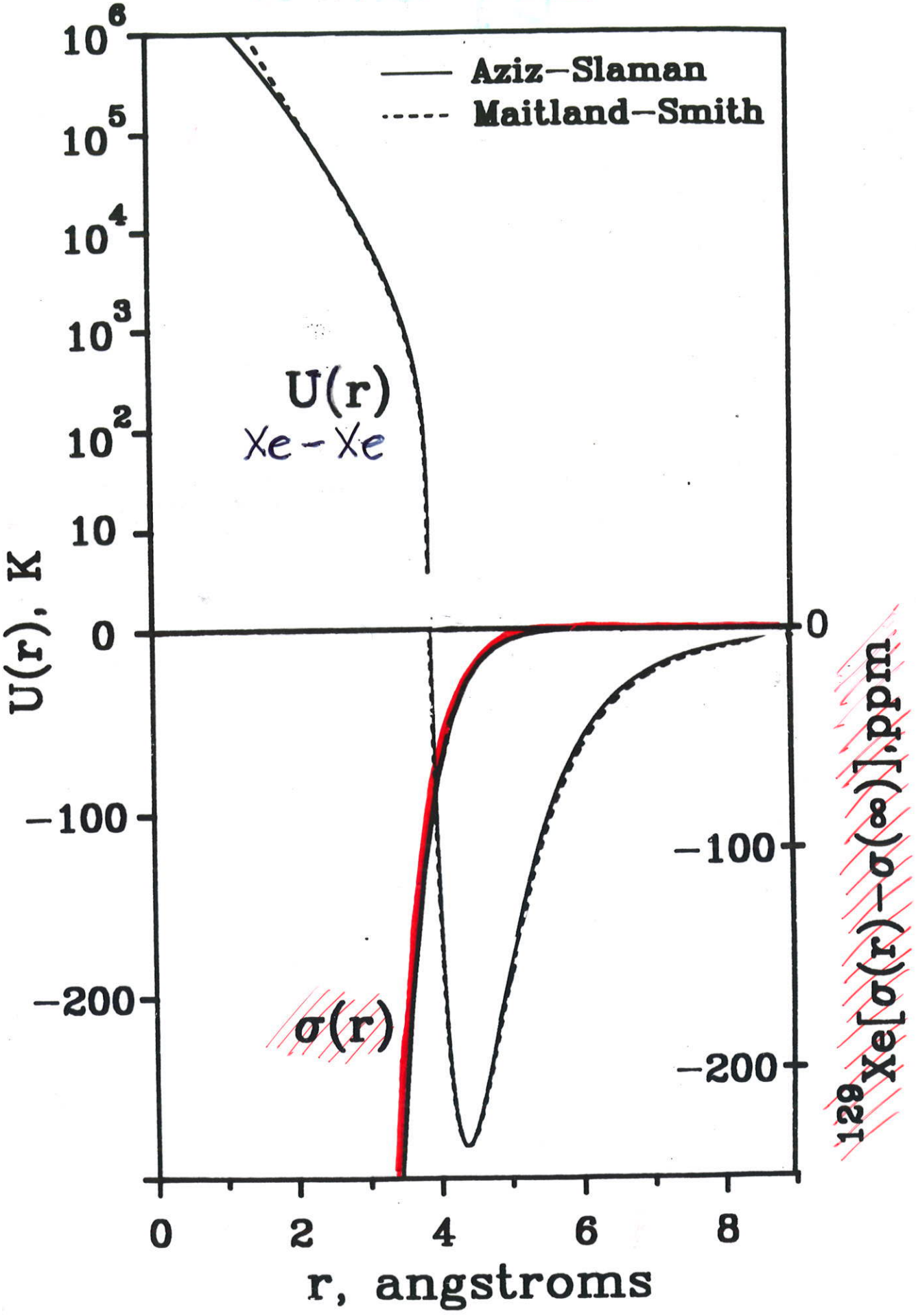
Aziz–Slaman
Maitland–Smith
U(r)
Xe – Xe
σ(r)
U(r), K
10^6
10^5
10^4
10^3
10^2
10
0
−100
−200
−100
−200
0
0
2
4
6
8
r, angstroms
^{129}Xe[σ(r)−σ(∞)], ppm

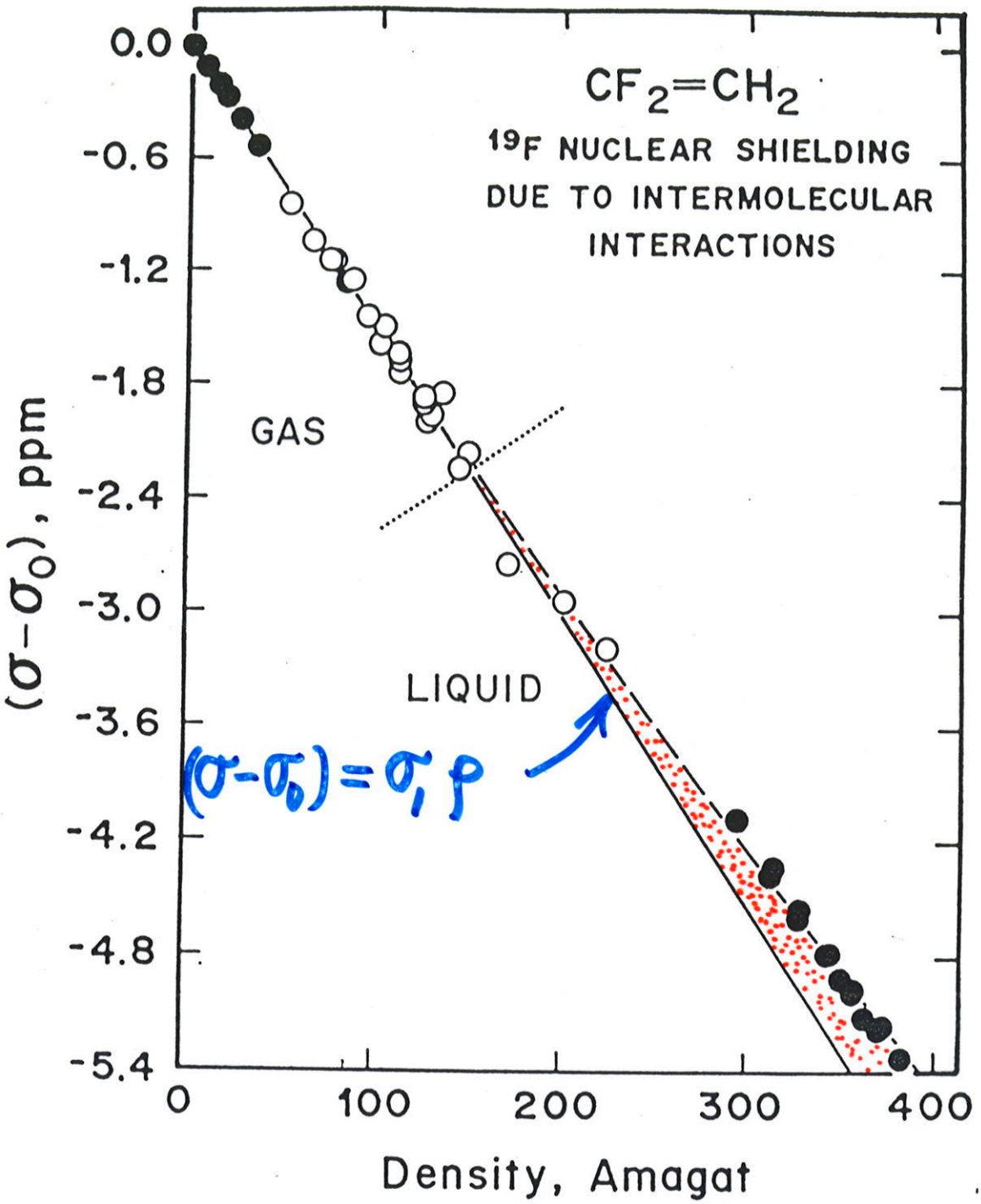

FIG. 3. The density dependence of the ^{19}F nuclear shielding. The filled circles are from this work, the open circles are from Wisman (Ref. 3). There was no observable temperature dependence of σ_1 obtained from the low density data shown in Fig. 1. Wisman's gas data taken at 305 K. The liquid data were taken at 293–303 K (Wisman) and 220–280 K (this work). The slope of the straight line is $-0.015\,22$ ppm amagat^{-1}. Densities of the liquid were obtained from Landolt–Börnstein, Vol IV 4 a. The critical point is 303.3 K, 146 amagat.

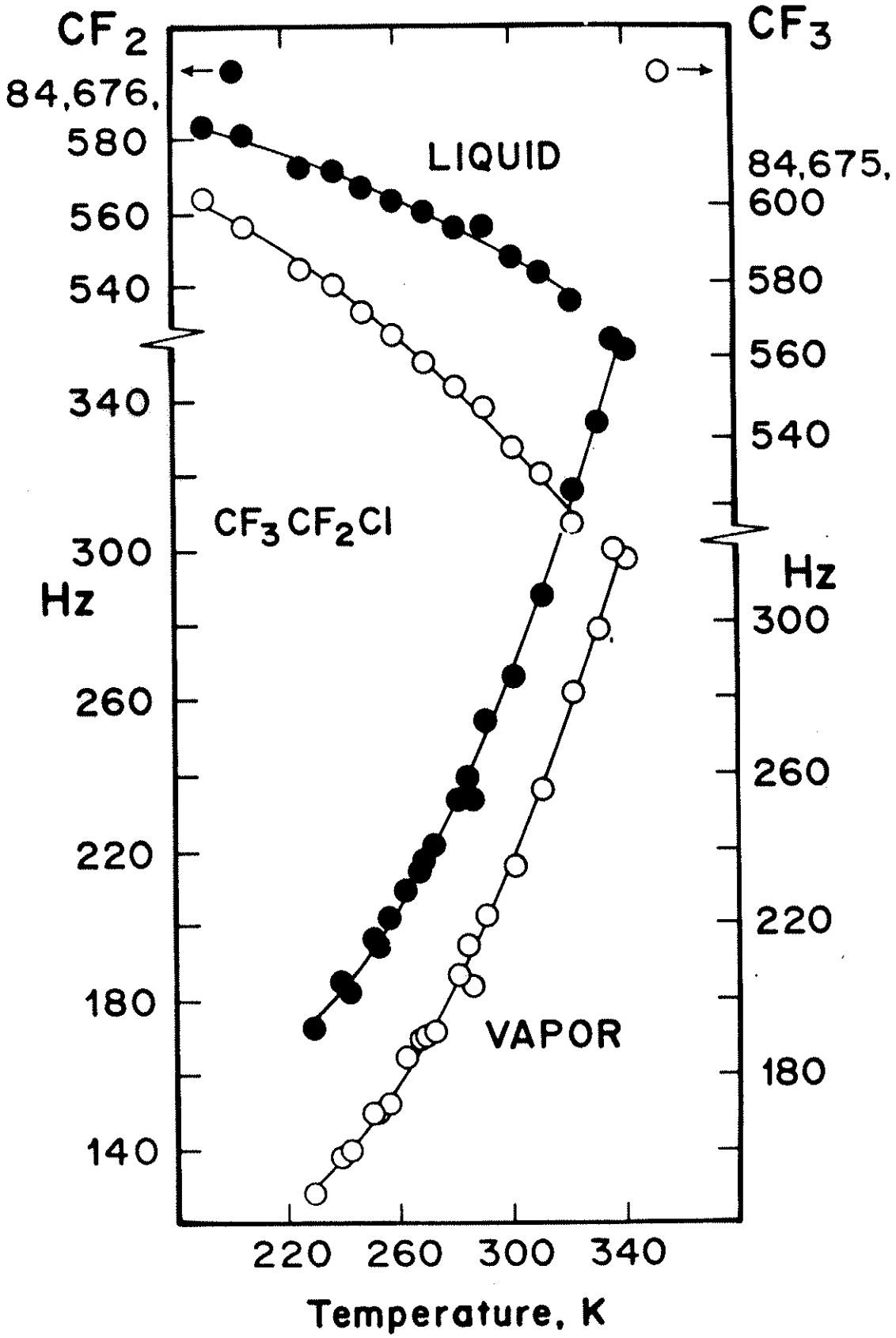
CF2
CF3
84,676,
580
560
540
340
300
260
220
180
140
Hz
84,675,
600
580
560
540
300
260
220
180
Hz
LIQUID
CF3CF2Cl
VAPOR
220
260
300
340
Temperature, K

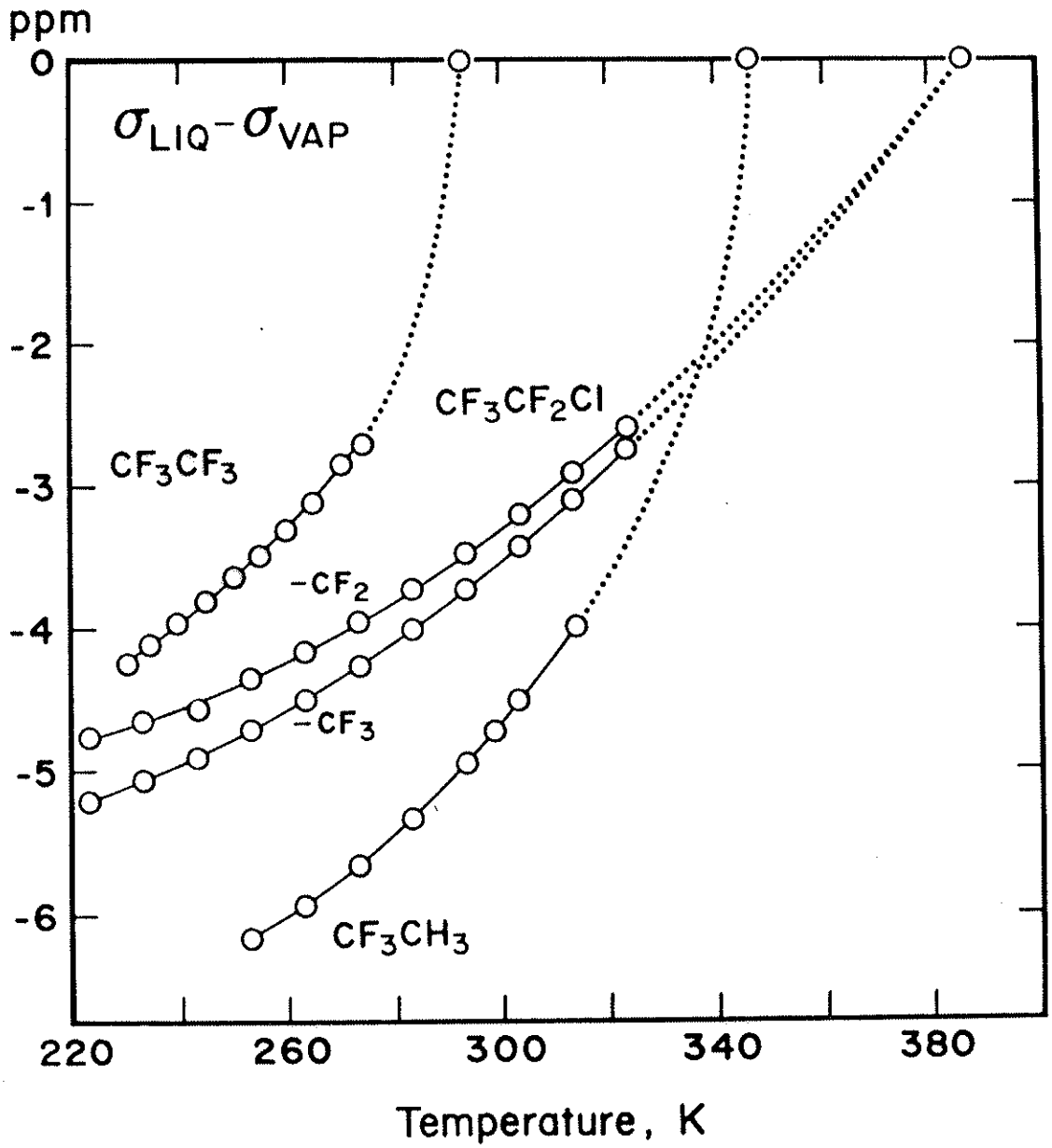
ppm
0
-1
-2
-3
-4
-5
-6
$\sigma_{LIQ} - \sigma_{VAP}$
CF_3CF_3
CF_3CF_2Cl
$-CF_2$
$-CF_3$
CF_3CH_3
220
260
300
340
380
Temperature, K

site factor

density coefficient of shielding in a gas is

$$\sigma_1(T) = \int \sigma(\mathbf{R}) \exp[-V(\mathbf{R})/k_B T] d\mathbf{R}$$

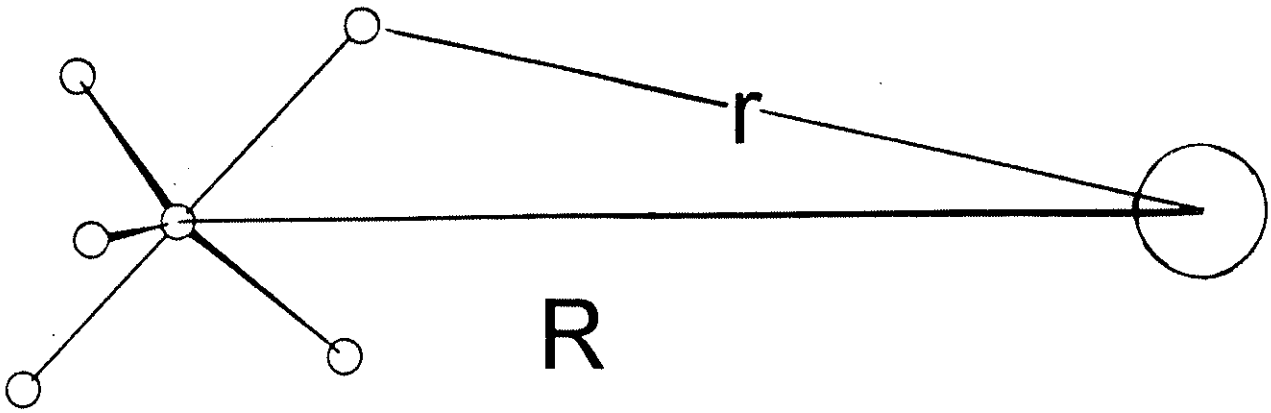

rare gas pairs: $\sigma_1(T) \sim \langle R^{-6} \rangle$

molecules with structure:

$\sigma_1(T) \sim \langle r^{-6} \rangle$ not $\langle R^{-6} \rangle$

$\sigma_1(T) \sim$ (site factor)$\langle R^{-6} \rangle$

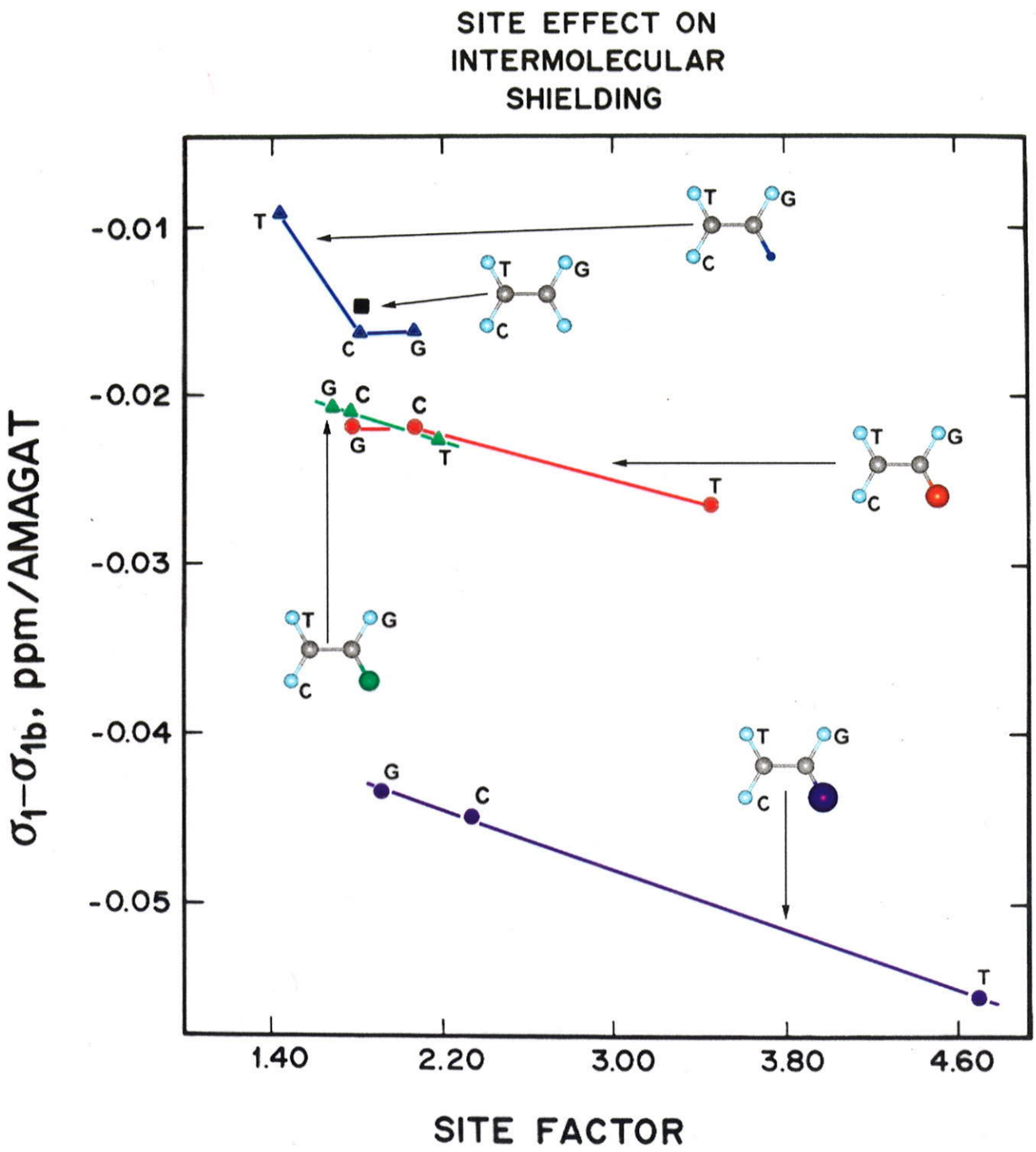
SITE EFFECT ON
INTERMOLECULAR
SHIELDING
-0.01
-0.02
-0.03
-0.04
-0.05
$\sigma_1 - \sigma_{1b}$, ppm/AMAGAT
1.40
2.20
3.00
3.80
4.60
SITE FACTOR
T
G
C

- When molecules are adsorbed in a microporous solid at a given loading, how are these molecules distributed among the cavities?

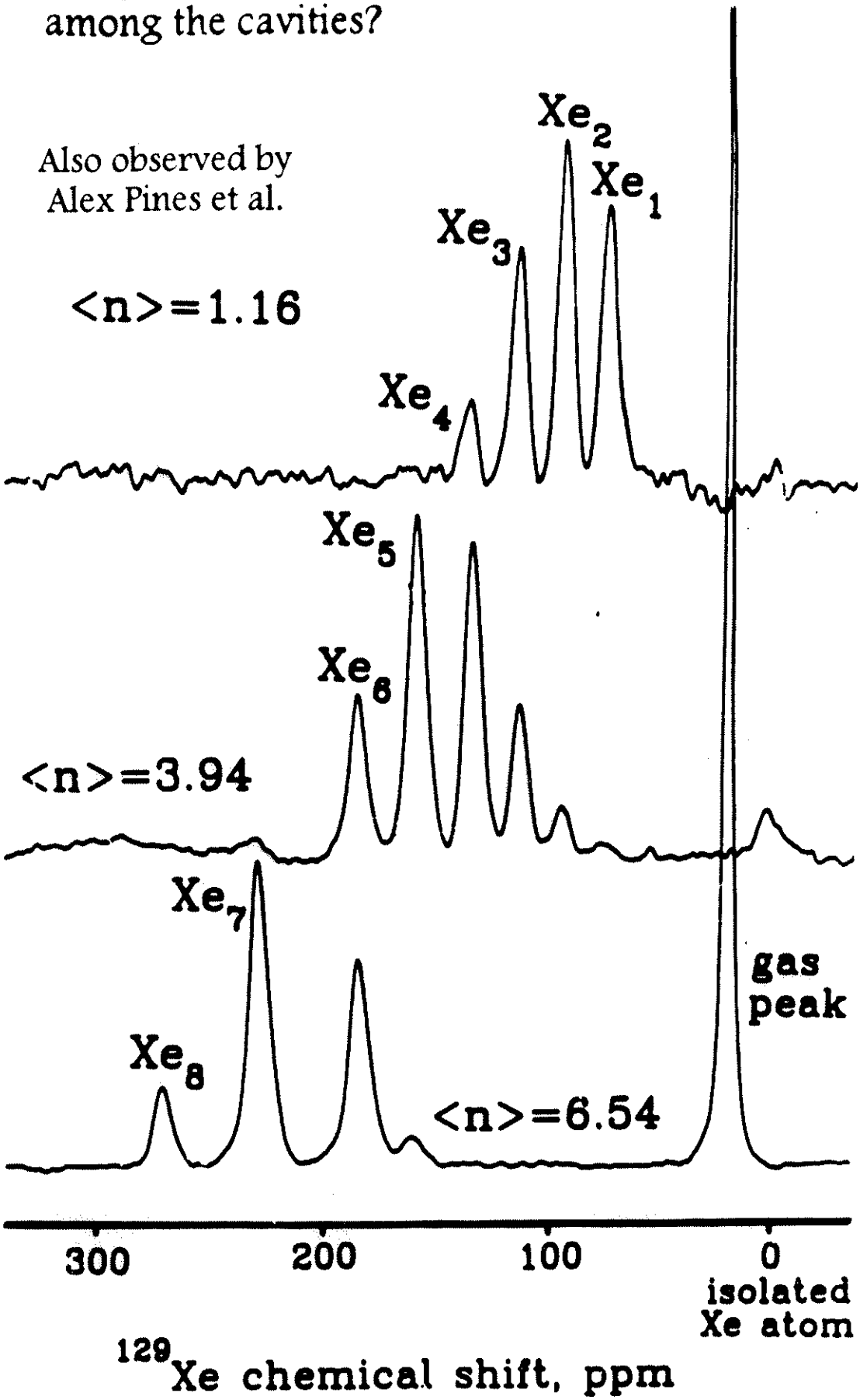

Temperature dependence of ^{129}Xe chemical shift at near-zero loading

Xe in NaY (0.25 Xe/supercage)

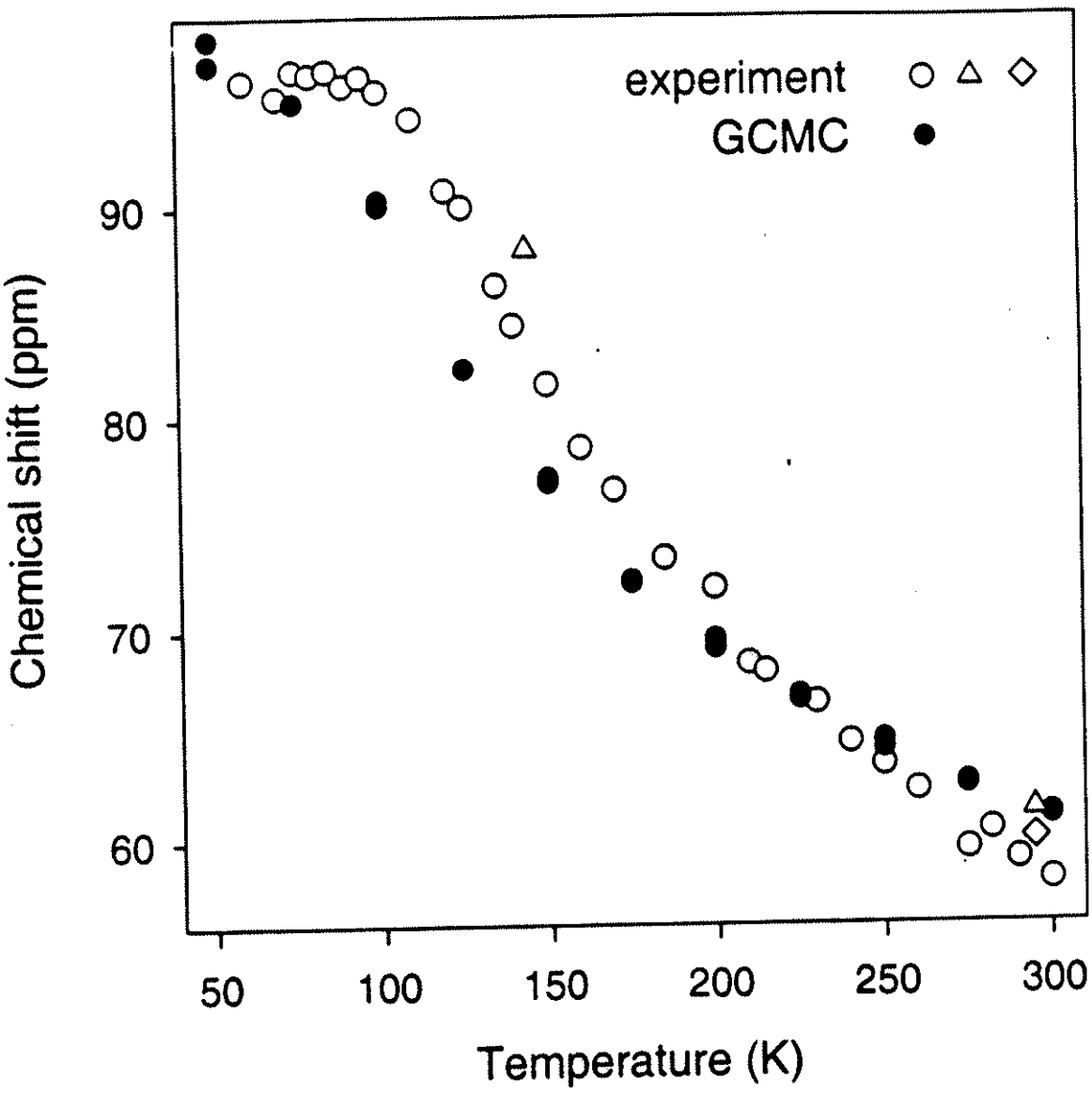

Experiments from Labouriau, Pietrass, Weber, Gates, and Earl.

"Ring Currents"

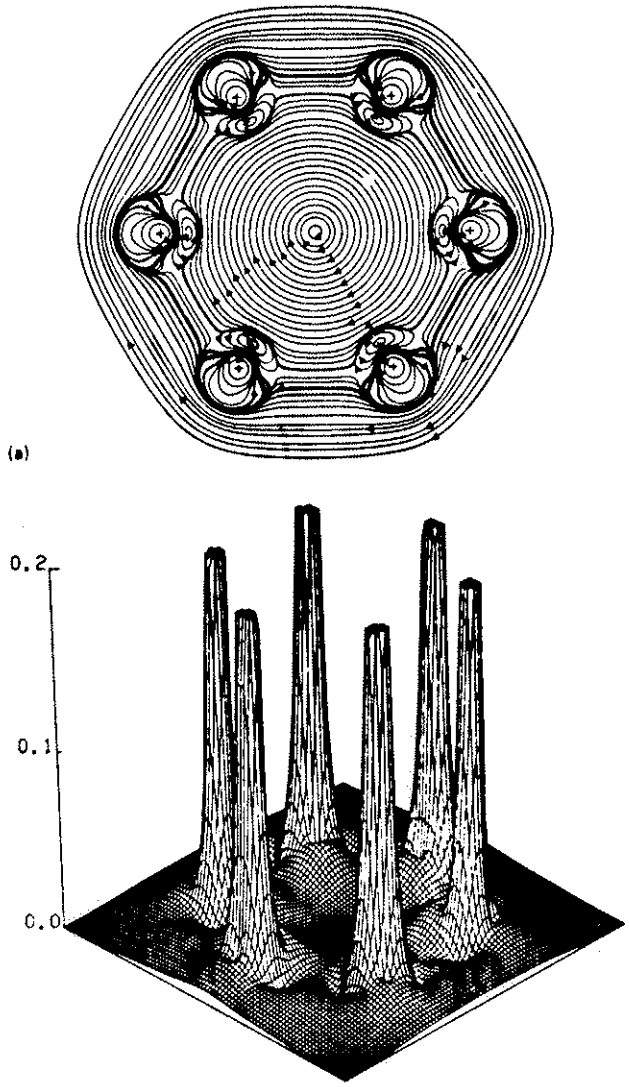

Streamlines of current density on the molecular plane of Li_6. The presence of a topological loop, resulting from ring closure implies the existence of closed circuits, i.e., of ring currents. It is NOT , by itself, sufficient to guarantee that they have large intensity, which is the essential fact needed to explain magnetism of aromatic systems. In cyclic molecules like benzene the interplay of pi distortivity and sigma driving force provide a unique phenome nology. [P. Lazzeretti, Prog. NMR Spectrosc. 2000, 36, 1-88]

"Ring Currents"

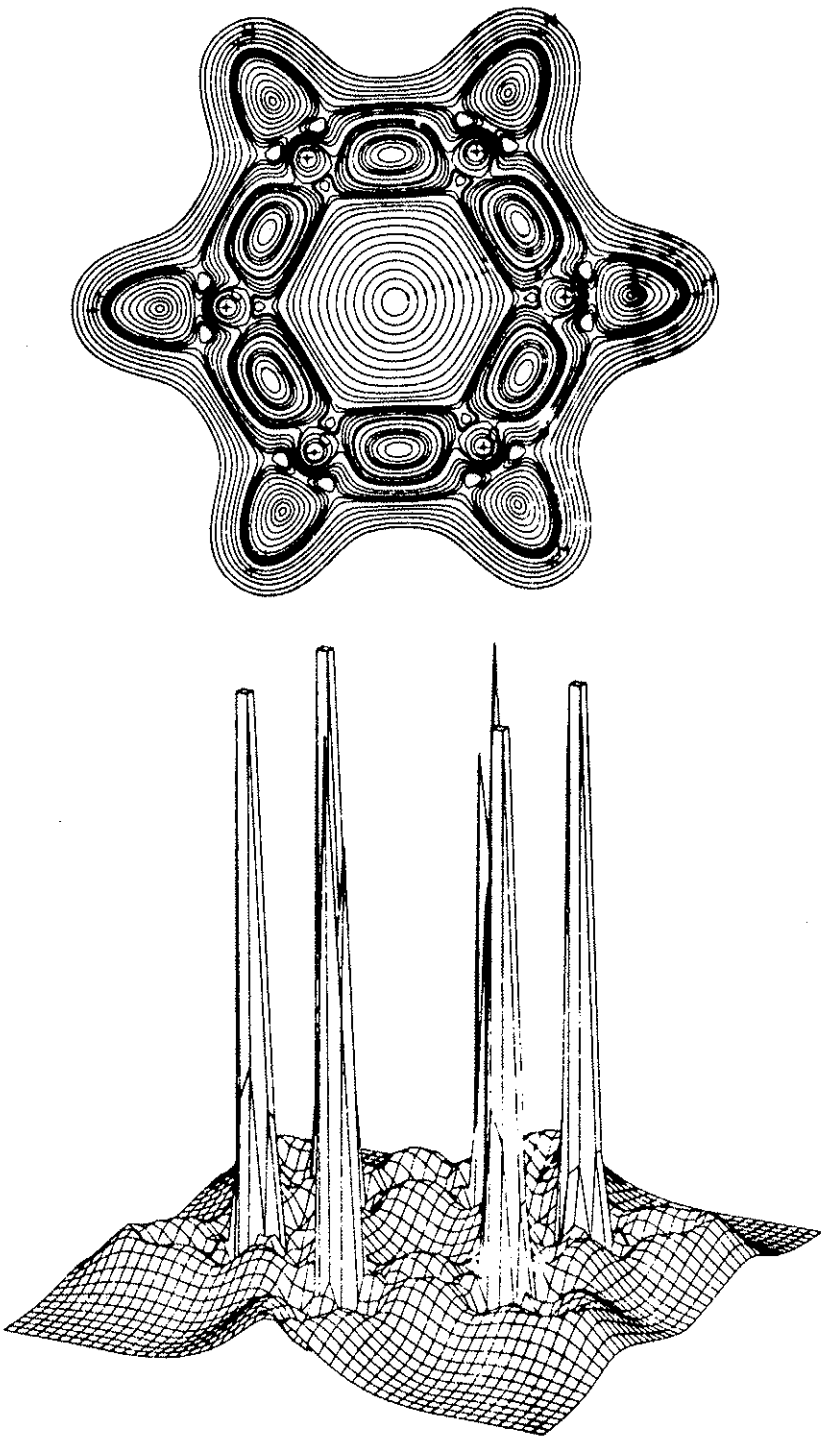

Streamlines of current density on the molecular plane of benzene [P. Lazzeretti, *Prog. NMR Spectrosc.* 2000, 36, 1-88, P. Lazzeretti, R. Zanasi, *J. Chem. Phys.* 1981, 77, 3129]

"Ring Current" Shielding @ Benzene

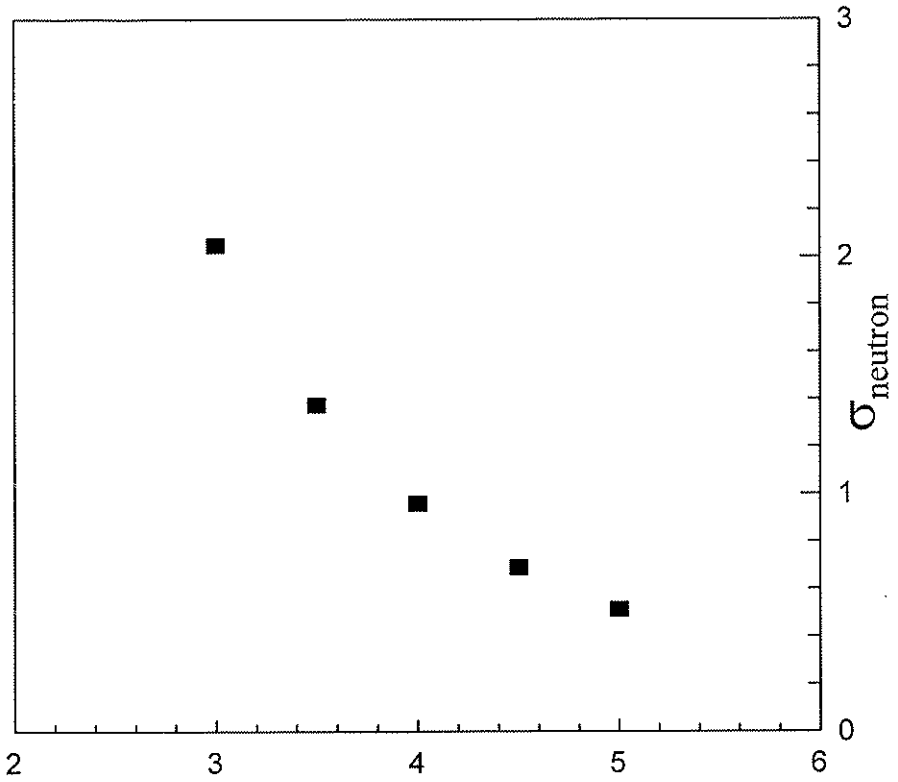

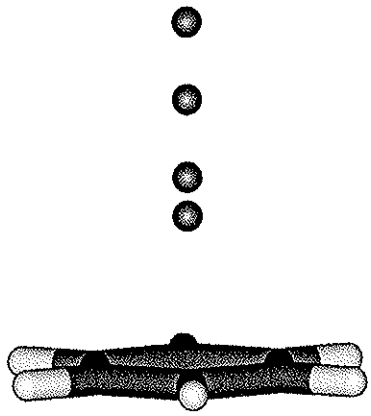

"Ring Current" Shielding @ Channel

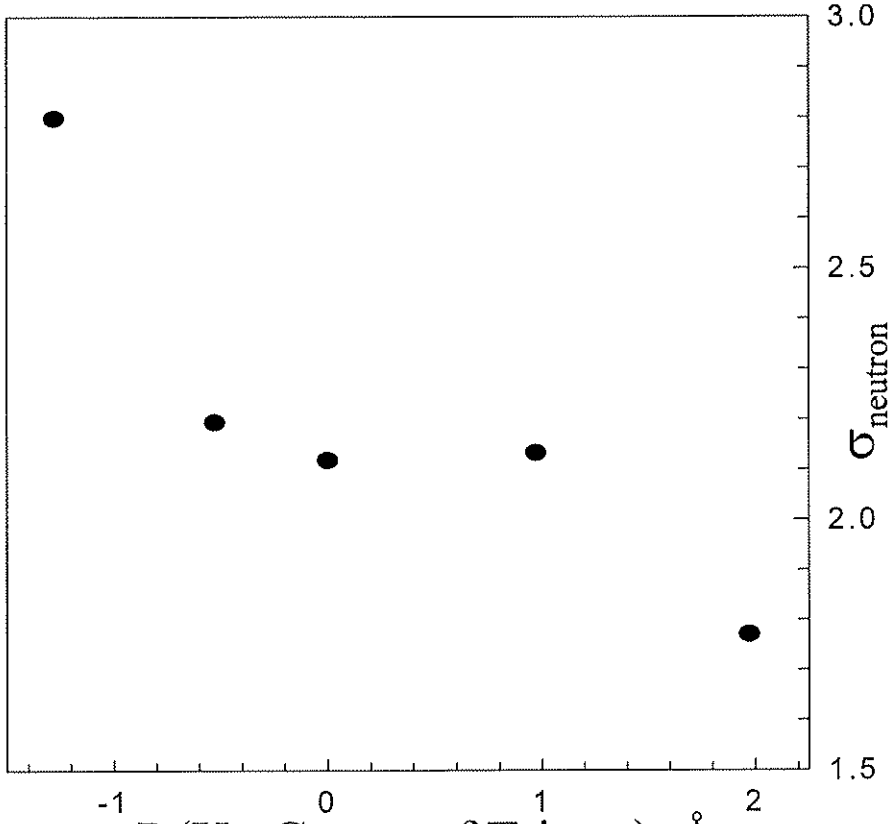

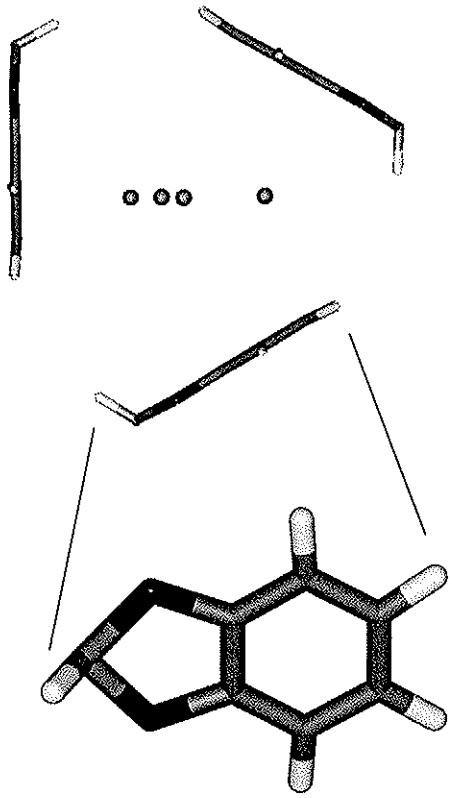

“Ring currents” inside C_{60} and other fullerenes

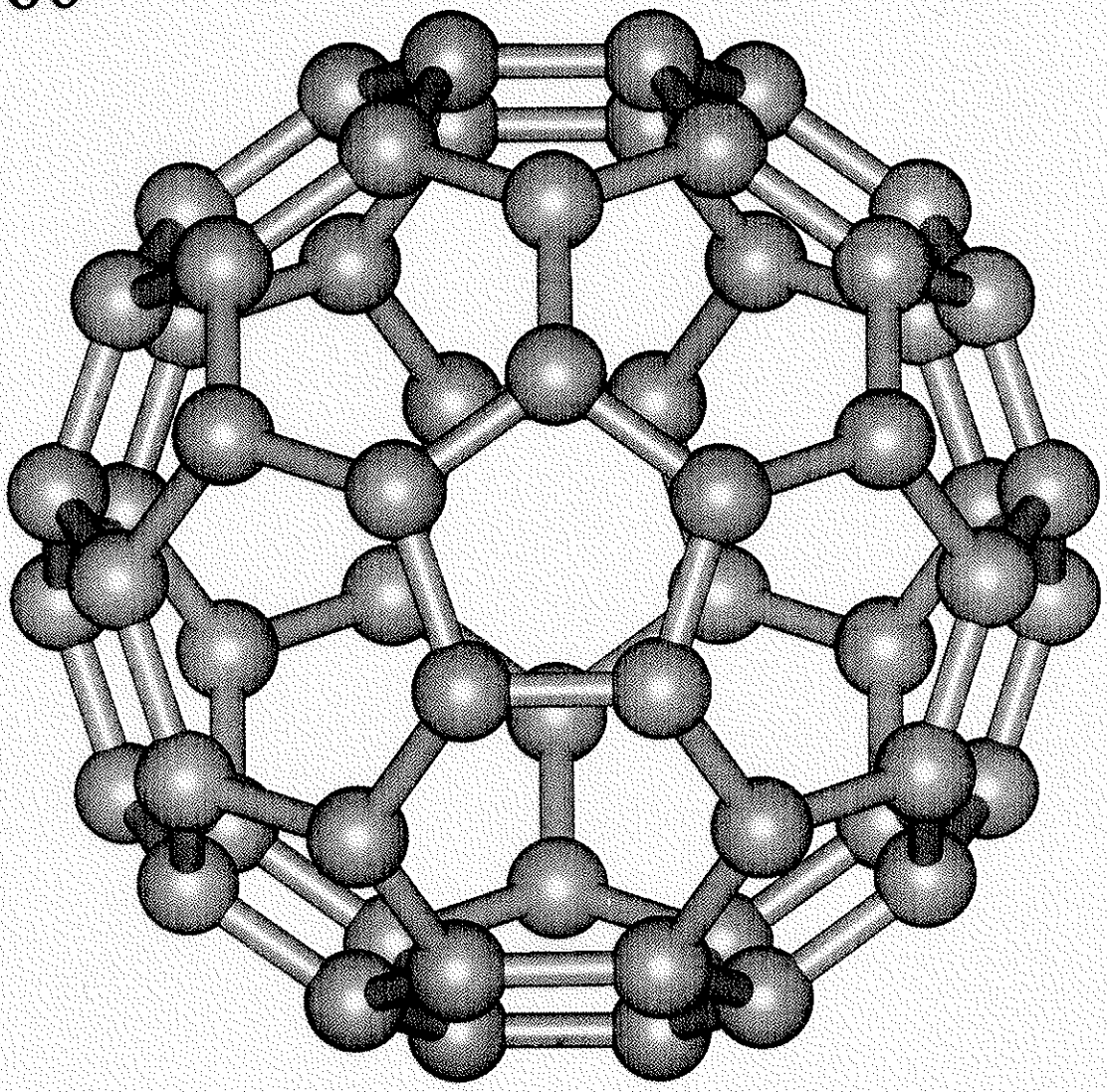

"Ring Currents in C_{60}"

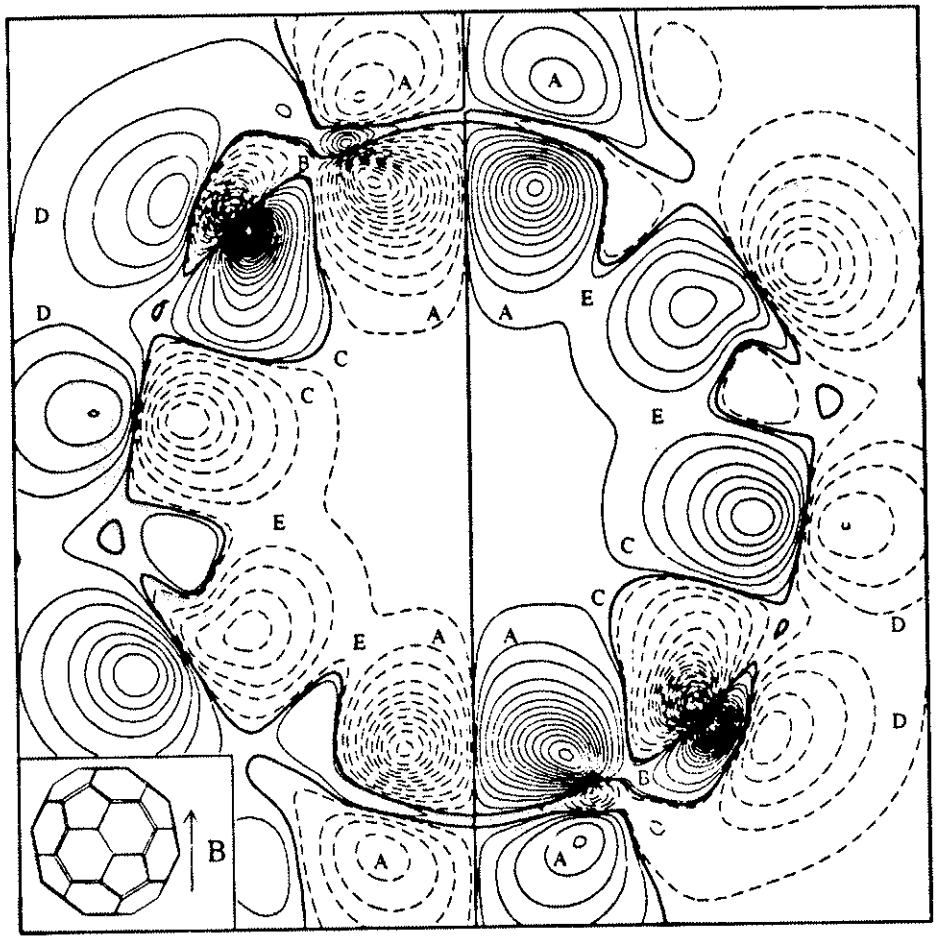

Induced pi electron currents in C_{60}, magnetic field B perpendicular to a pentagon

R. Zanasi, P. W. Fowler, Chem. Phys. Lett. 1995, 238, 270.

Any magnetic moment, a neutron, at the same location could measure the shielding response.

^{3}He nucleus in He atom experiences a shielding response that is almost the same as that for a neutron.

Thus, ^{3}He NMR spectroscopy provides us essentially the bare unamplified shielding at its location.

^{3}He in fullerenes

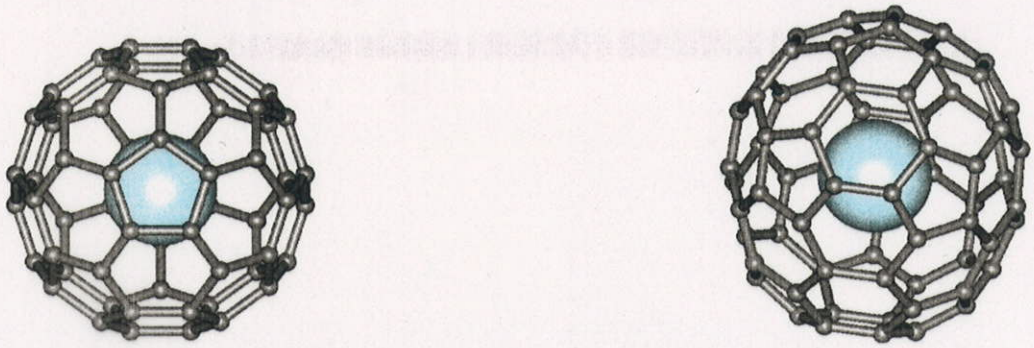

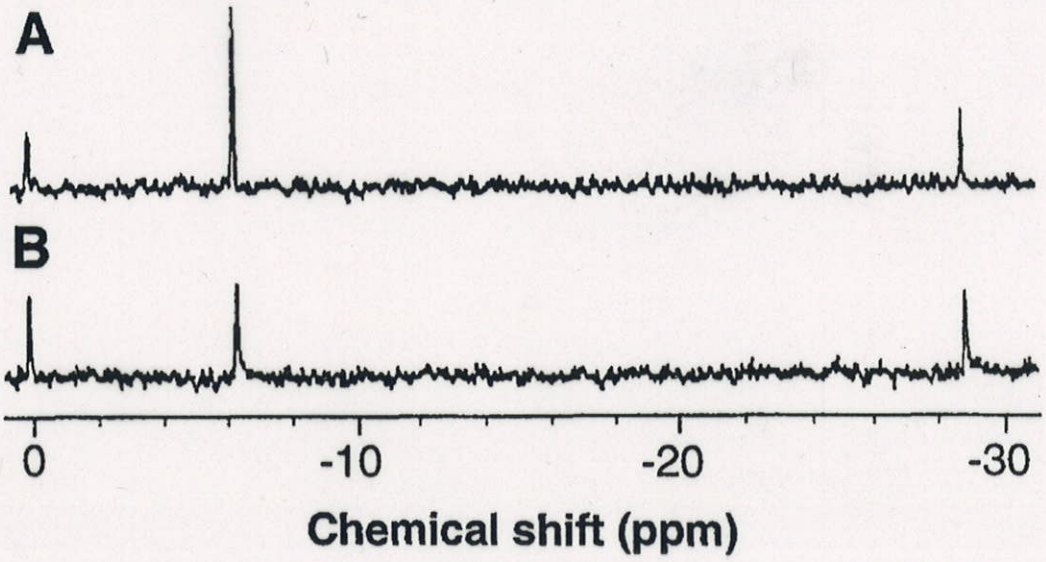

^{3}He NMR spectra of (**A**) a mixture of dissolved helium, C_{60}, and C_{70} and (**B**) the same mixture enriched in C_{70}.

Saunders M, Cross RJ, Jimenez-Vazquez HA, Shimshi R, and Khong A. Science. 271, 1693-1697. **1996**.

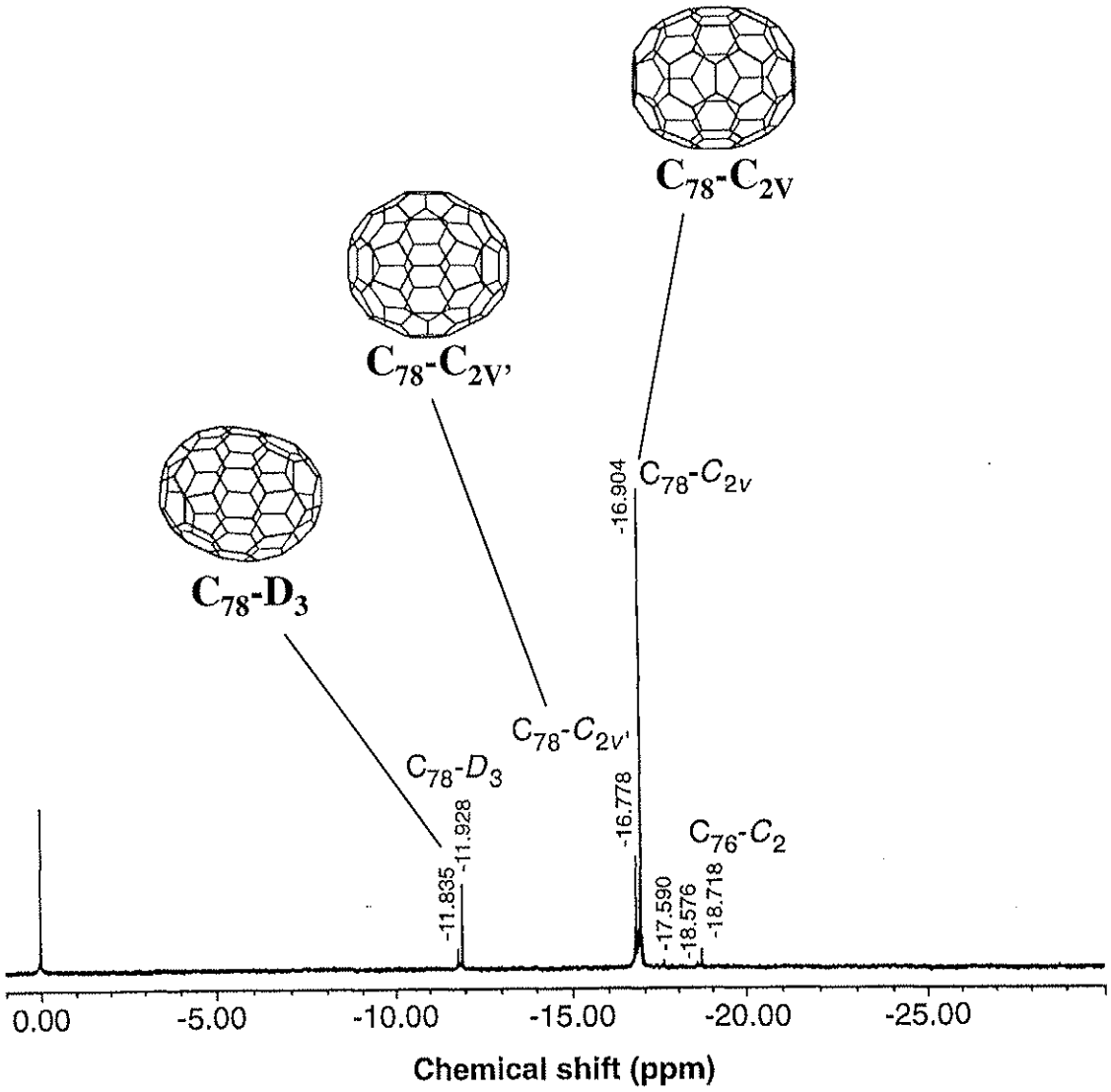

^{3}He NMR spectra of the higher fullerenes C_{76} and C_{78}.

Saunders M, Cross RJ, Jimenez-Vazquez HA, Shimshi R, and Khong A. Science. 271, 1693-1697. **1996**.

Saunders M, Jimenez-Vazquez HA, Cross RJ, Billups WE, Gessenberg C, Gonzalez A, Luo W, Haddon RC, Diederich F, and Herrmann A. J. Am. Chem. Soc. 117, 9305-9308. **1995**.

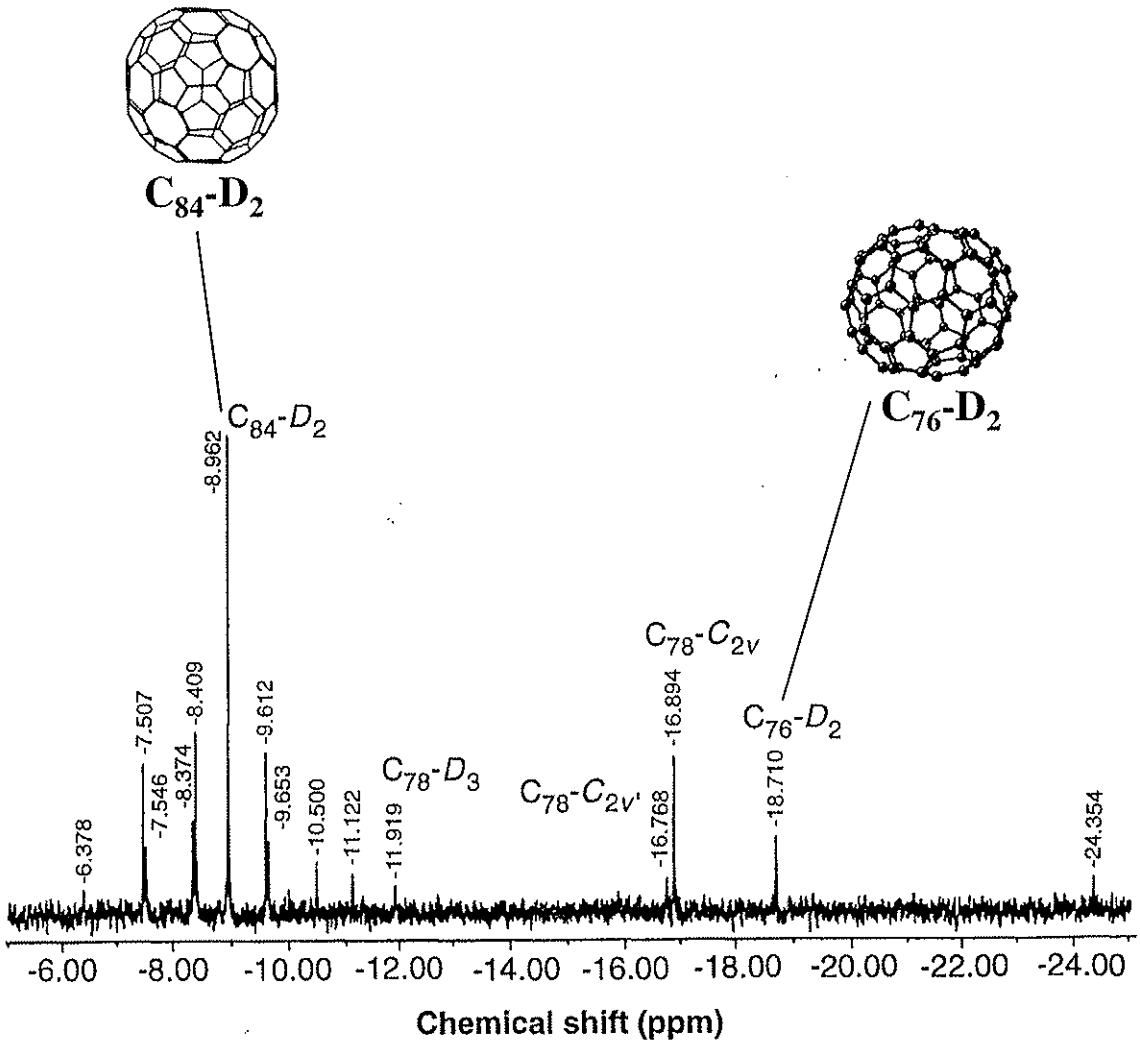

^{3}He NMR spectra of the higher fullerenes C_{76}, C_{78}, and C_{84}.

Saunders M, Cross RJ, Jimenez-Vazquez HA, Shimshi R, and Khong A. Science. 271, 1693-1697. **1996**.

Saunders M, Jimenez-Vazquez HA, Cross RJ, Billups WE, Gessenberg C, Gonzalez A, Luo W, Haddon RC, Diederich F, and Herrmann A. J. Am. Chem. Soc. 117, 9305-9308. **1995**.

^{3}He NMR spectra of C_{70} adducts shown on right. Chemical shifts are relative to free dissolved ^{3}He.

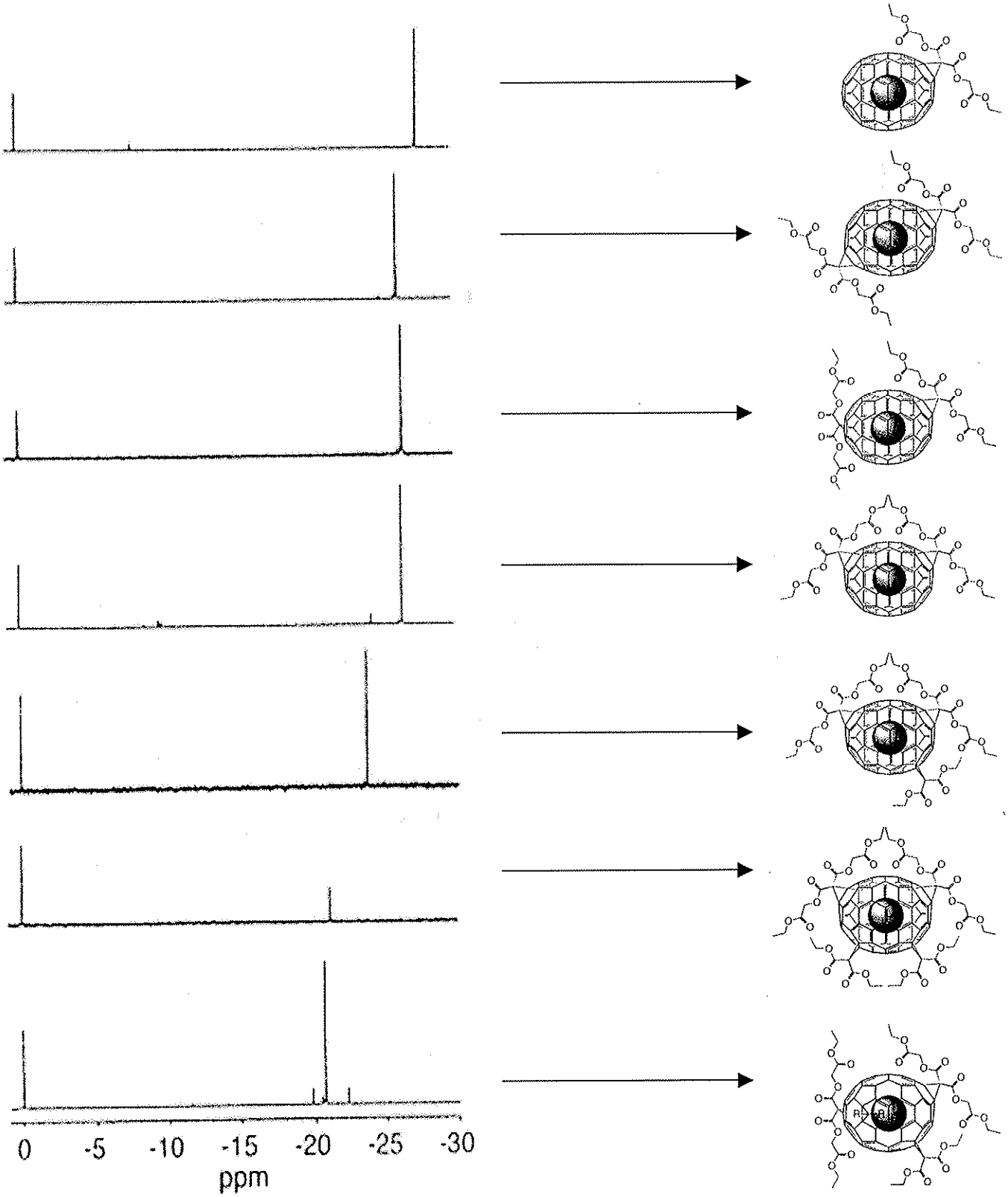

Ruttimann M, Haldimann R, Isaacs L, Diederich F, Khong A, Jimenez-Vazquez H, Cross RJ, Saunders M. Chem. Eur. J. 3, 1071-1076. **1997**.

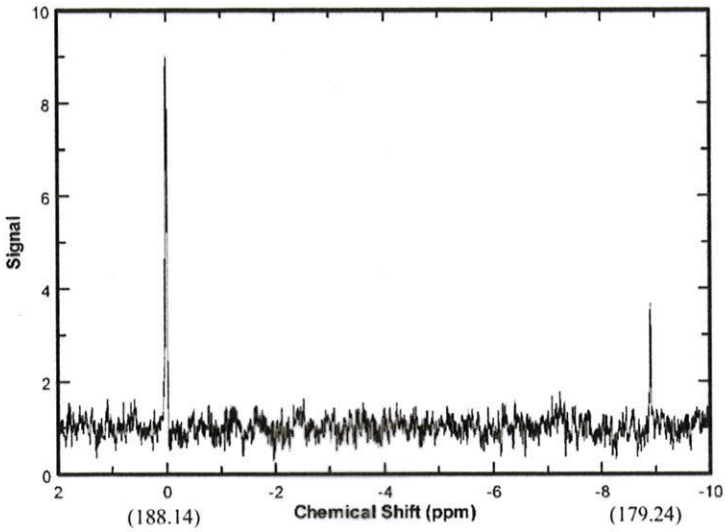

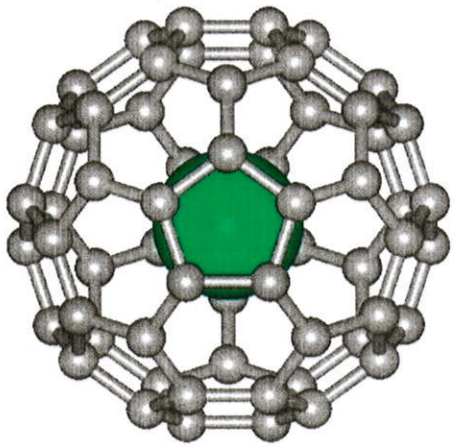

^{129}Xe NMR of ^{129}Xe@C_{60} (dissolved ^{129}Xe is the reference at 0 ppm).

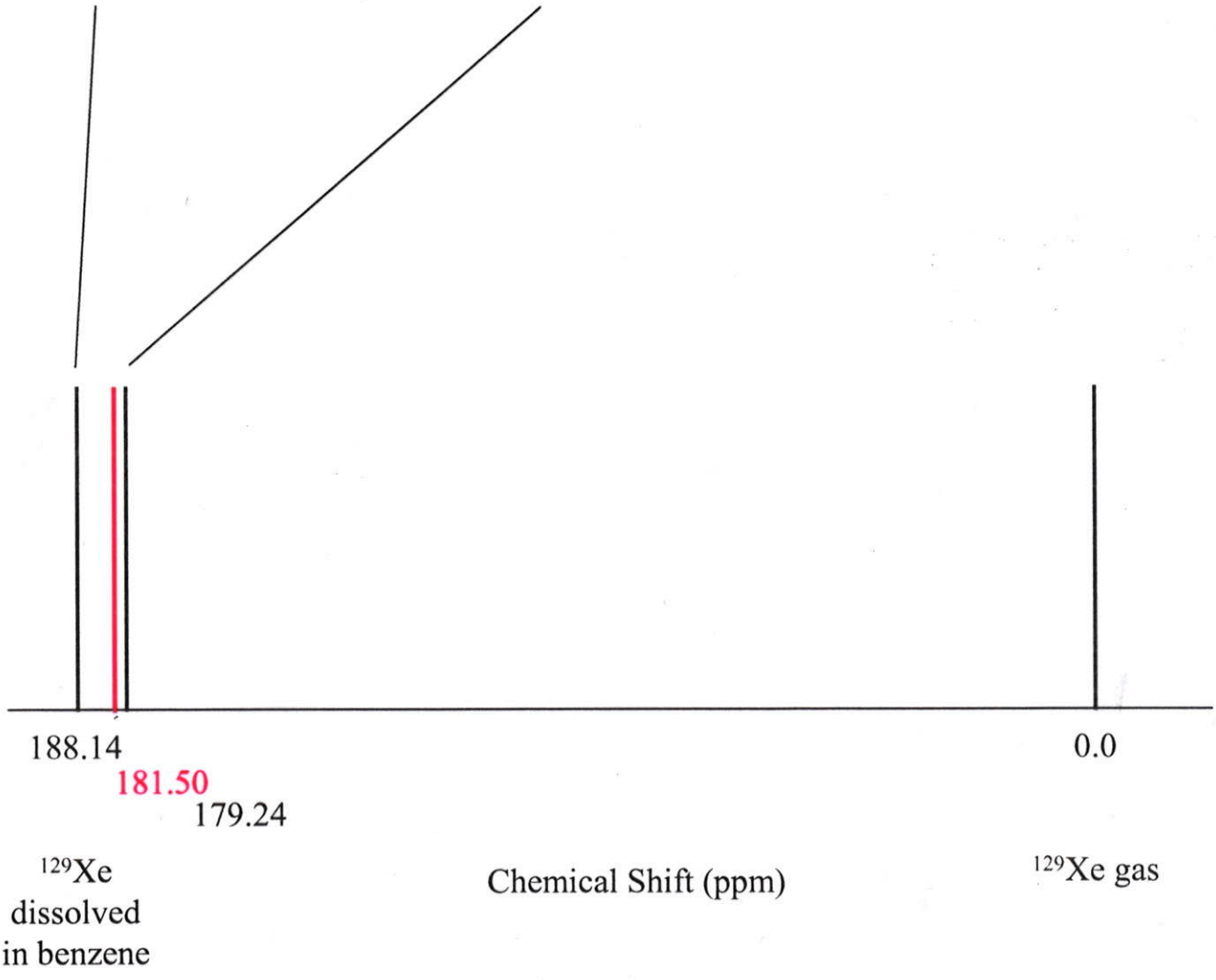

Syamala MS, Cross RJ, and Saunders M. J. Am. Chem. Soc. 124, 6216-6219. **2002**.

NMR chemical shift perturbation mapping of protein-protein interactions in solution

protein A

protein A in AB complex

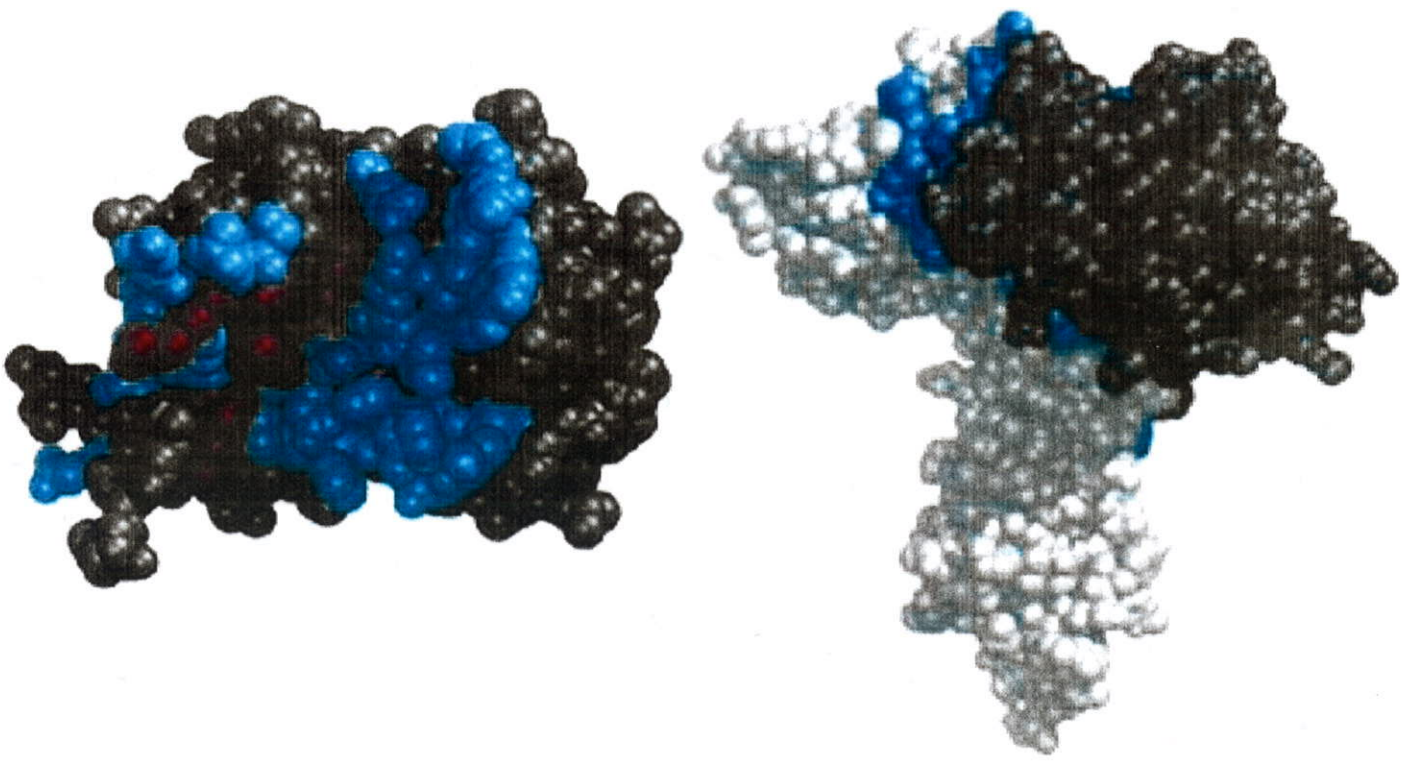

free state

bound state

The Chemical Shift Perturbation Method

Free State

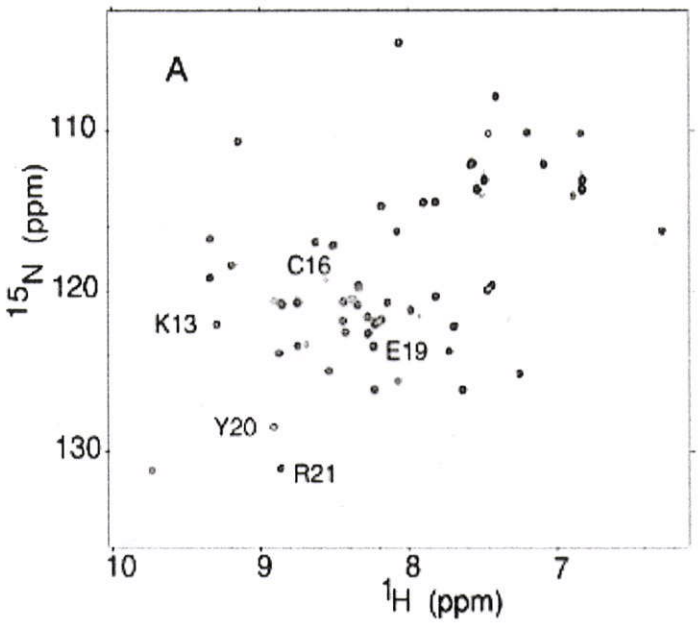

Bound State

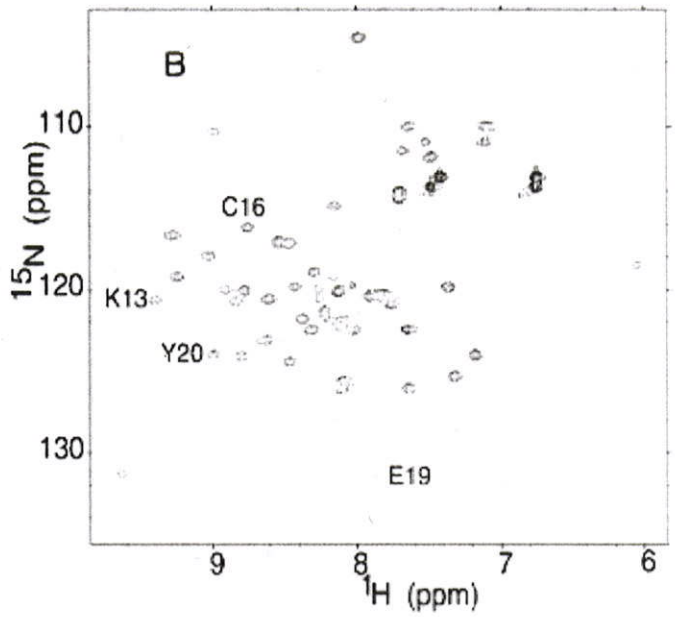

In Contact with Chymotrypsin:

From X-Ray

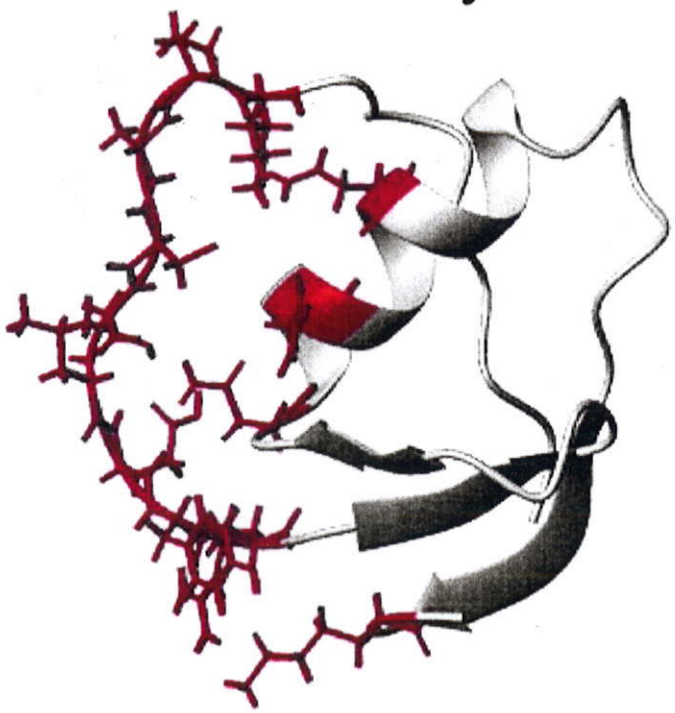

From NMR Chemical Shifts

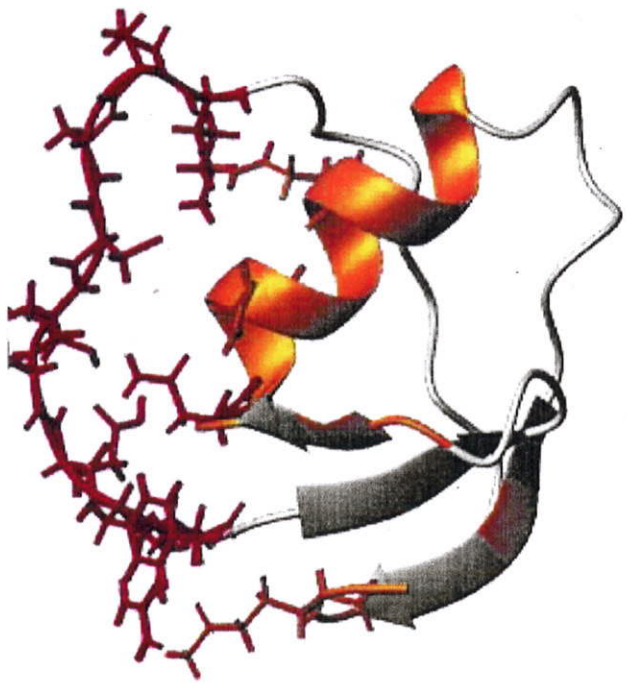

Song J, Markley JL. J. Mol. Recognit. 14, 166-171. **2001**.

Applications to Drug Design

Chemical shift changes observed on ligand binding can be used to screen candidate compounds in designing an inhibitor.

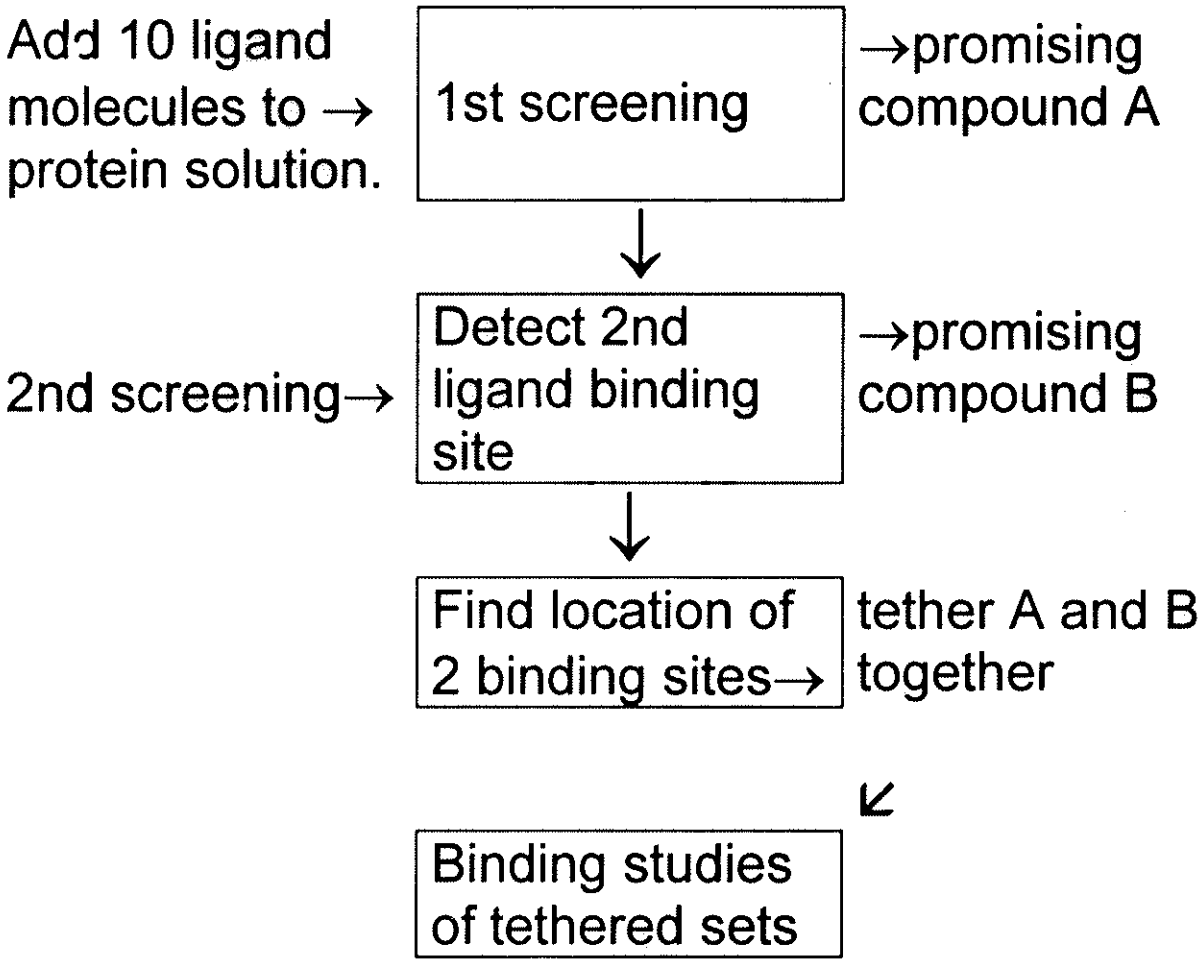

A tight binding inhibitor may be found by tethering together two weak binding inhibitors.

S. W. Fesik et al. *Science* 1996, 1997

Motivation:

Xe as a biosensor (Pines, Wemmer, et al. 2001)

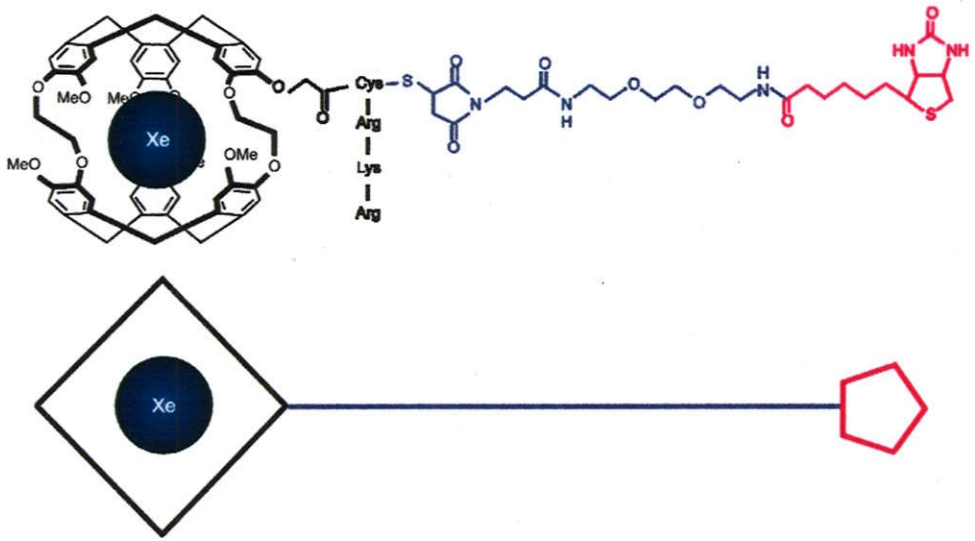

Experiments on Xe in cryptophane cages provide model systems for comparison

- 2 unique cages A and E
- Temperature dependence of Xe @cryptoA
- Xe Isotope shifts upon deuteration of cage

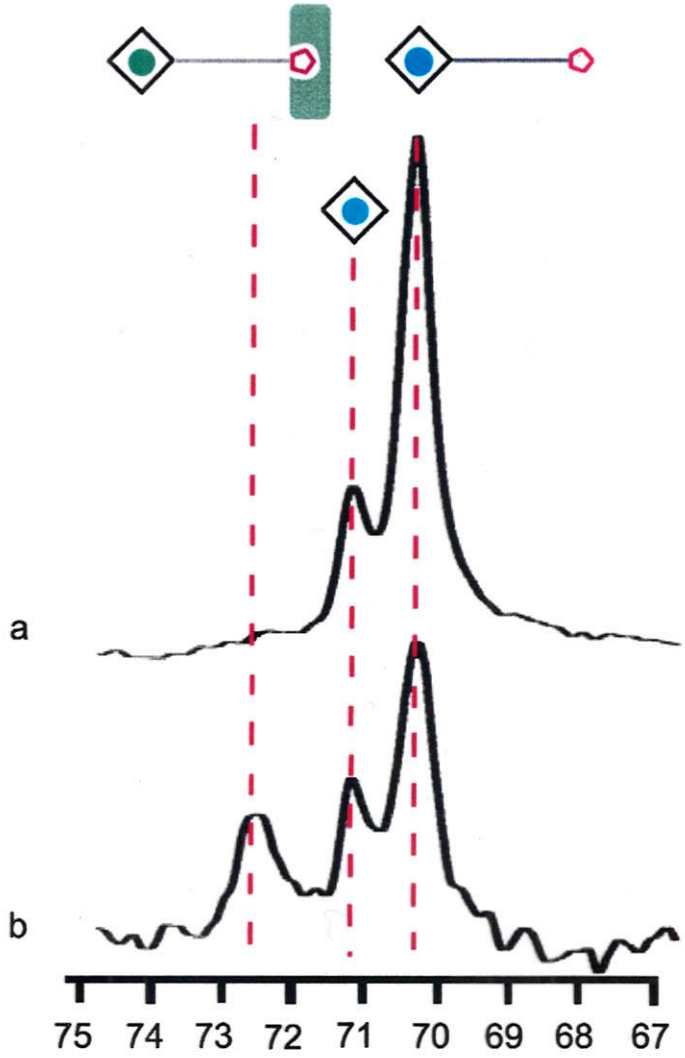

M.M. Spence, S.M. Rubin, I.E. Dimitrov, E.J. Ruiz, D.E. Wemmer, A. Pines, S.Q. Yao, F. Tian, and P.G. Schultz Proc. Nat. Acad. Sci. **2001**, 98, 10654-10657.

Cryptophanes

- Two cyclotriveratrylene bowls
- Connected by aliphatic linker $(CH_2)_n$
- n=2 Cryptophane-A (cryptoA)
- n=3 Cryptophane-E (cryptoE)

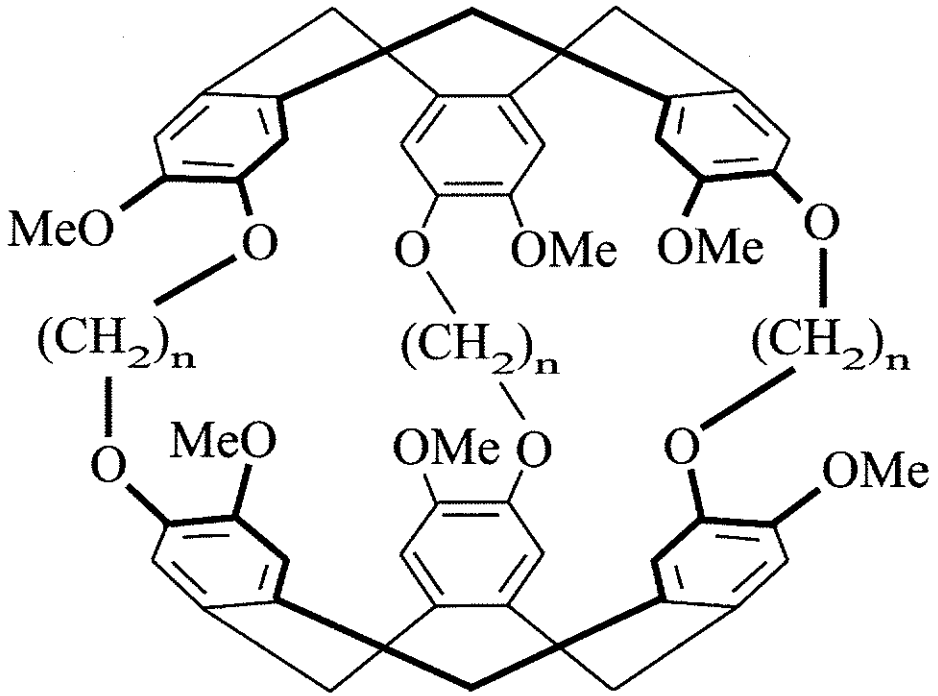

- To calculate average Xe chemical shifts:
- Solution structure of cryptoA and cryptoE (not the same as X-Ray structure)
- Suitable fragment for ab initio calculation of xenon shielding surface

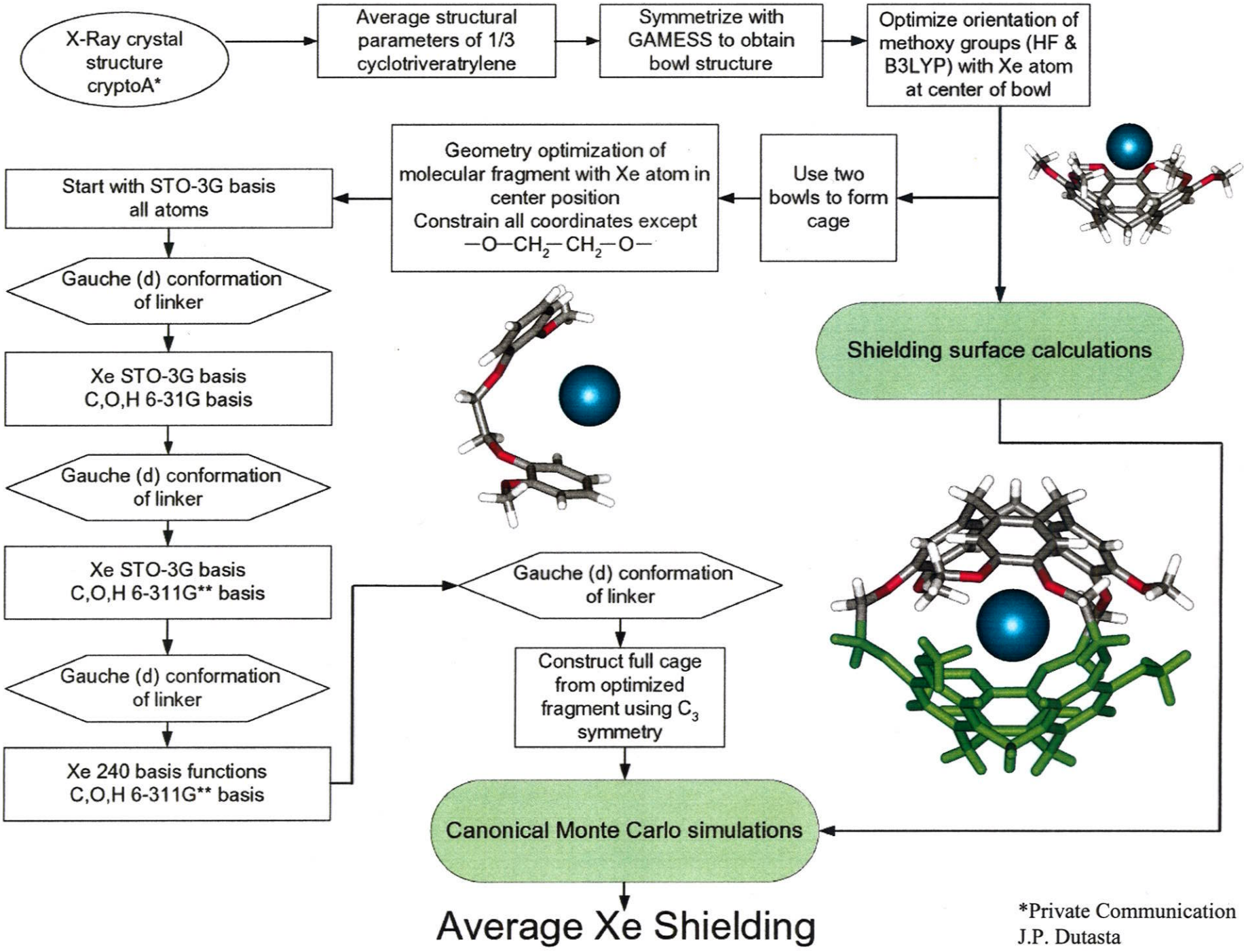

*Private Communication
J.P. Dutasta

The average structure of Xe@cryptoA to be used for Monte Carlo Simulations

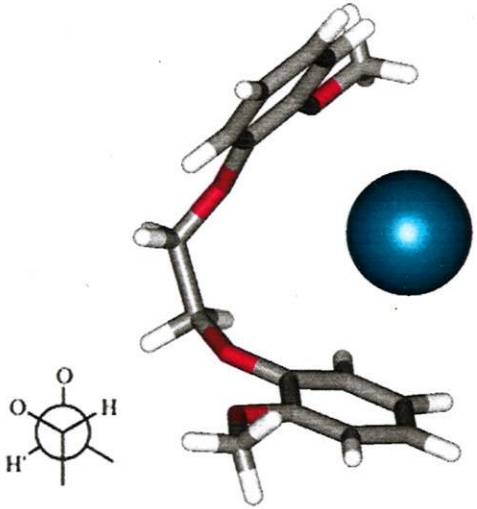

(d) conformation

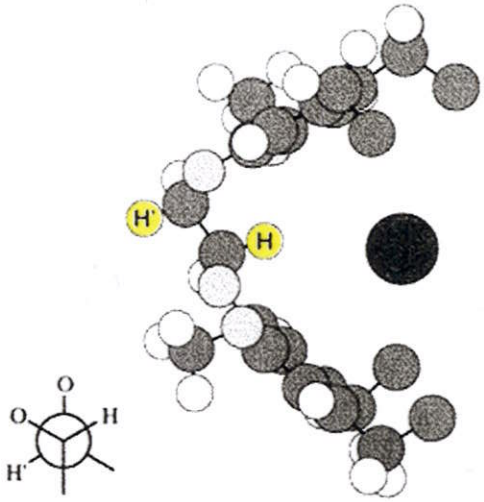

Pines et al. 1999*

(d) conformation

Minimum energy structure arrived at is completely consistent with SPINOE experiments by Pines et al!

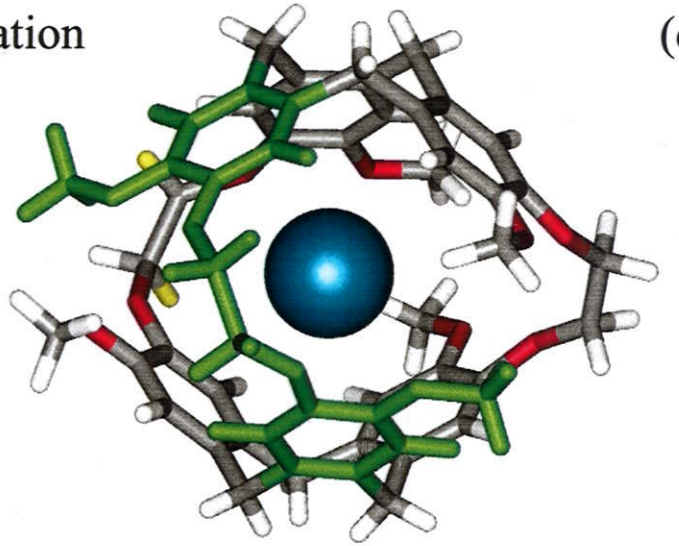

* M., Luhmer, B.M. Goodson, Y.Q. Song, D.D. Laws, L. Kaiser, M.C. Cyrier, and A. Pines J. Am. Chem. Soc. **1999**, 121, 3503-3512.

Xe shielding surface calculations in the model fragment

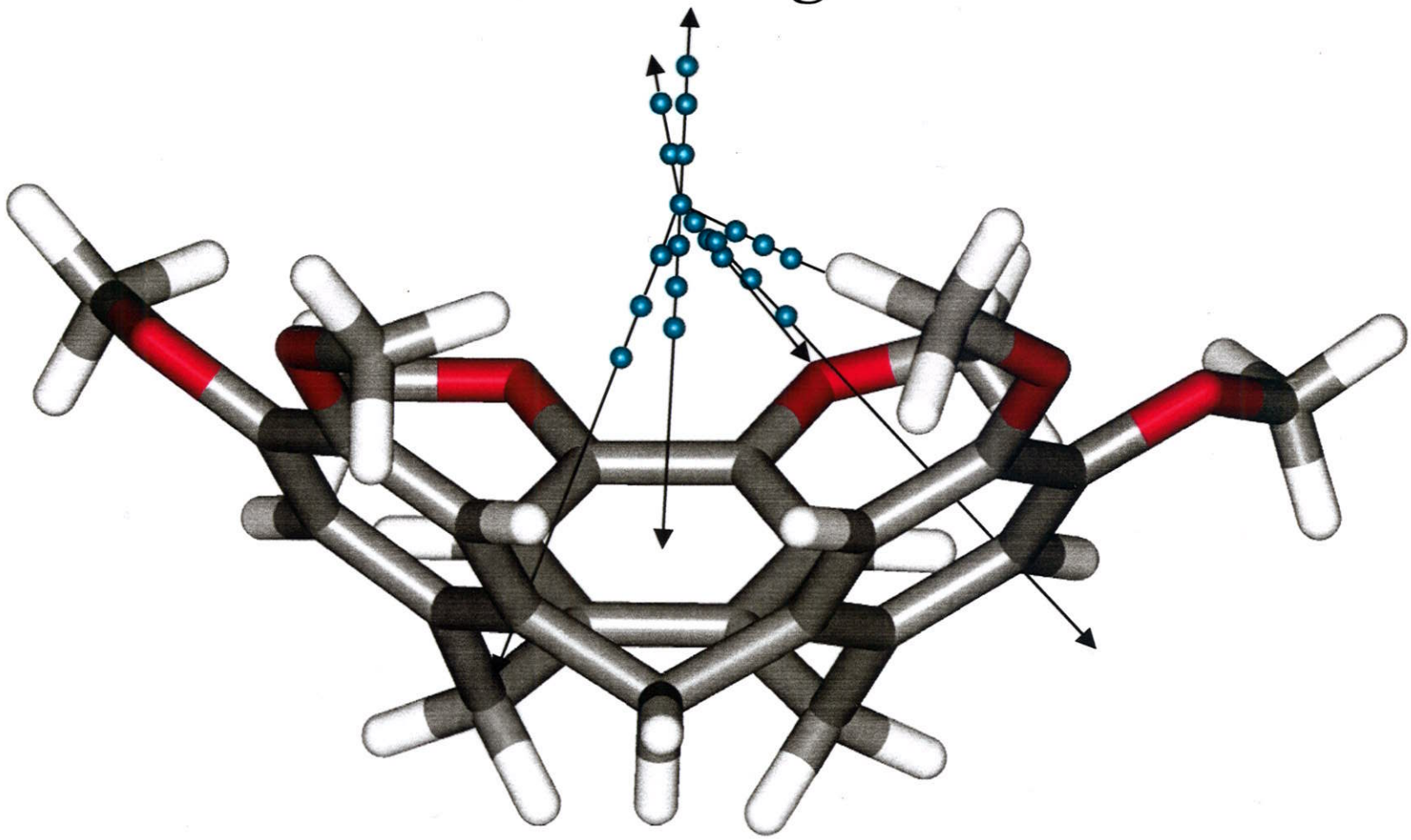

- Single cyclotriveratrylene
- Hartree-Fock and DFT (B3LYP)
- 6-311G** basis set on C,O, and H atoms
- 240 basis functions on Xe atom

The Xe shielding surface

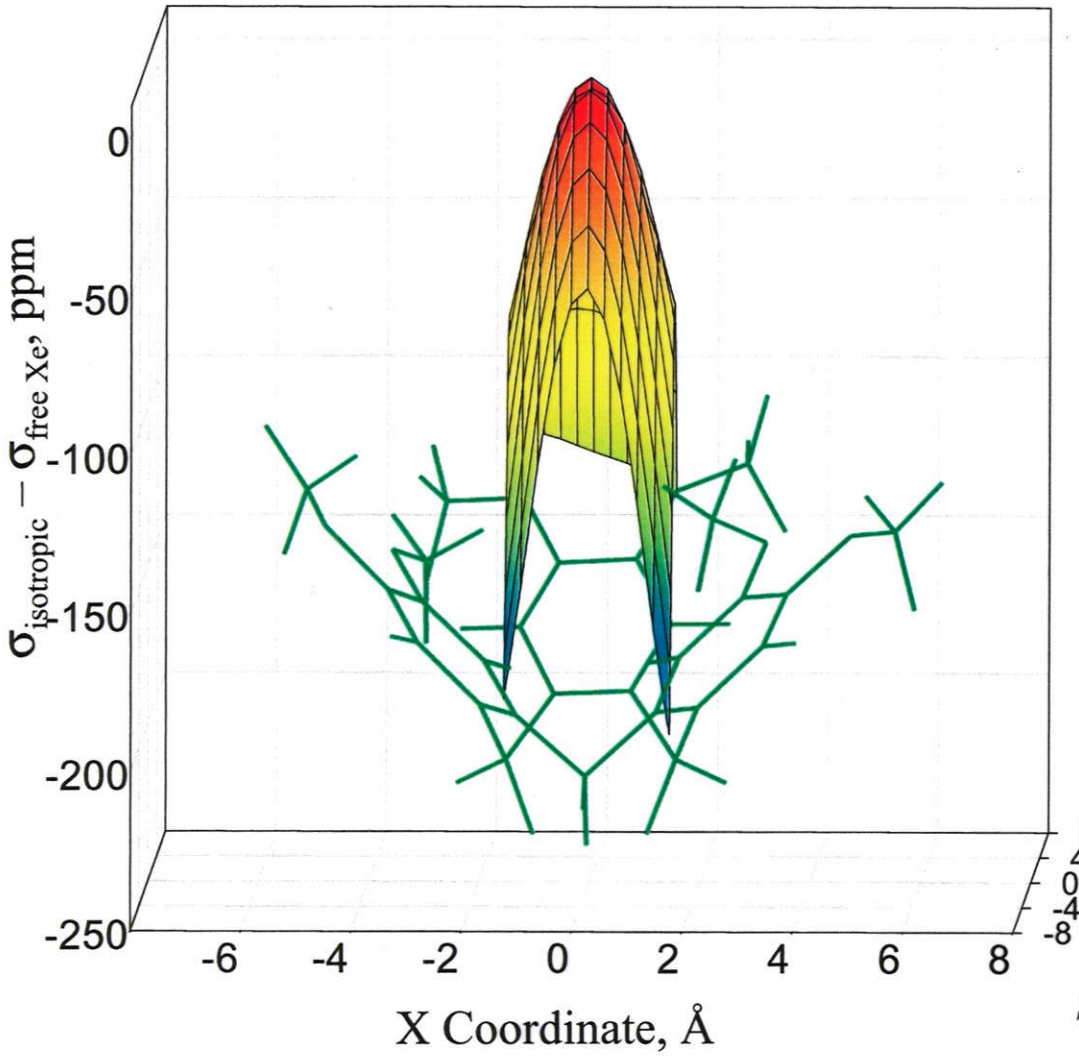

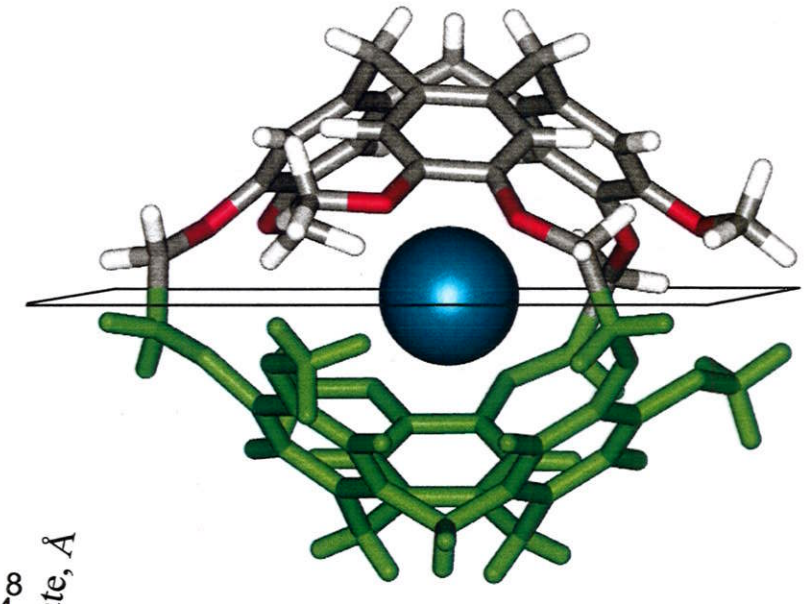

Monte Carlo simulations:
One-body distribution function for Xe@cryptoA

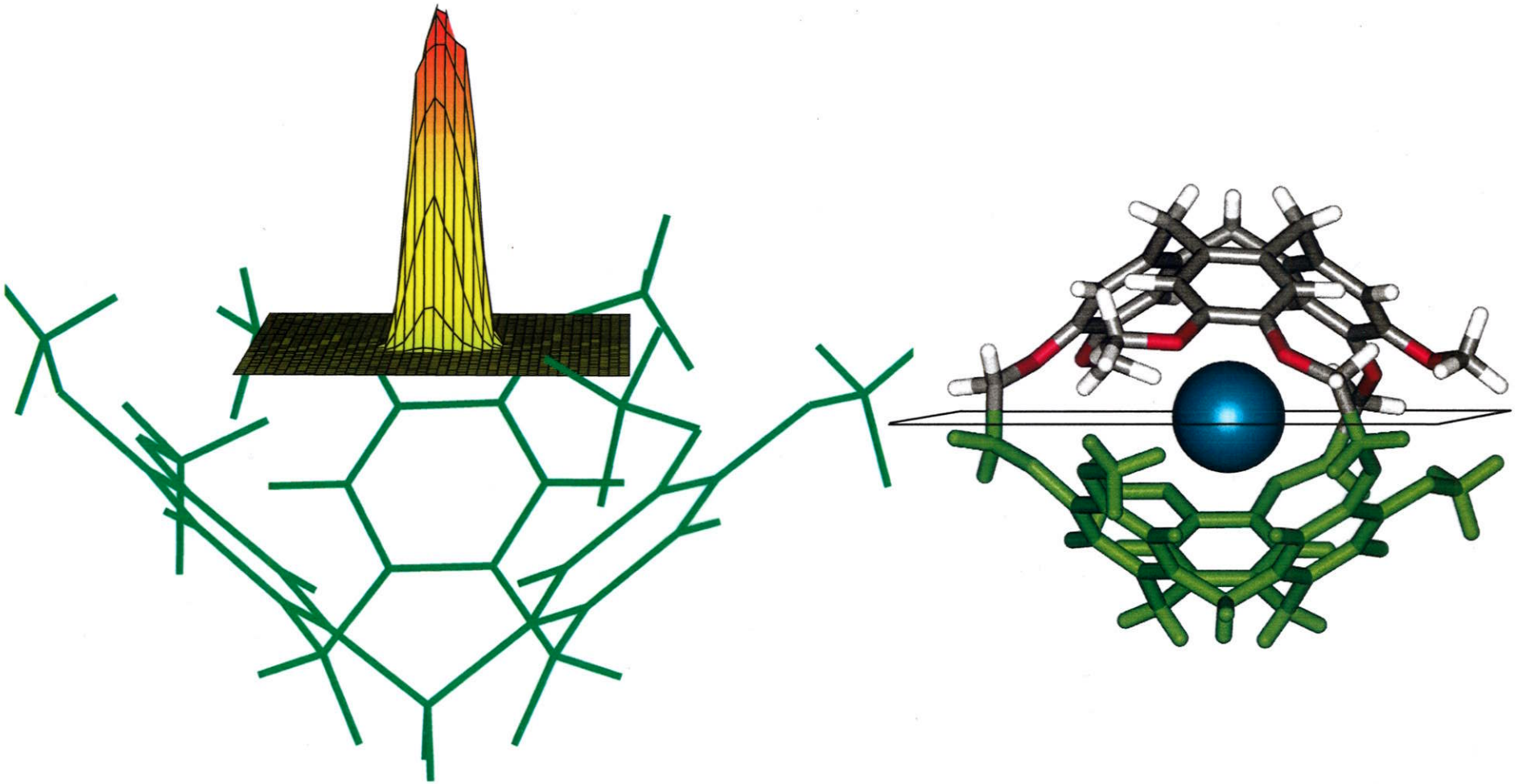

Monte Carlo average shielding for Xe@cryptoA

δ(ppm) relative to free Xe atom

*EXPT. (Brotin et al. 2000)	67.0
MC (this work)	60.46

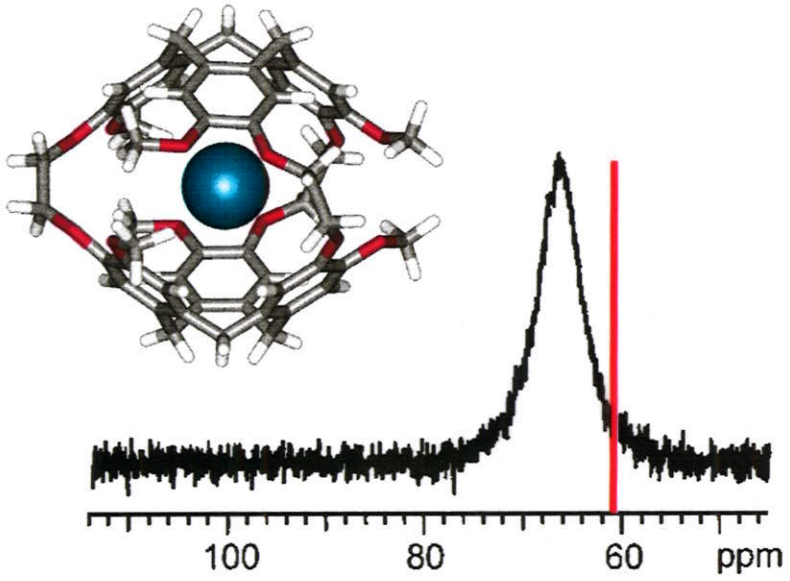

•Accept/reject displacements of xenon atom within the cage according to:

$P_{acc} = \min [1, \exp(-\Delta U_{config}/k_B T)]$

ΔU_{config} change in configurational energy

*T. Brotin, A. Lesage, L. Emsley, and A. Collet J. Am. Chem. Soc. **2000**, 122, 1171-1174
K. Bartik, M. Luhmer, J.P. Dutasta, A Collet, and J. Reisse J. Am. Chem. Soc. **1998**, 120, 784-791

Average structures of Xe@cryptoA and Xe@cryptoE

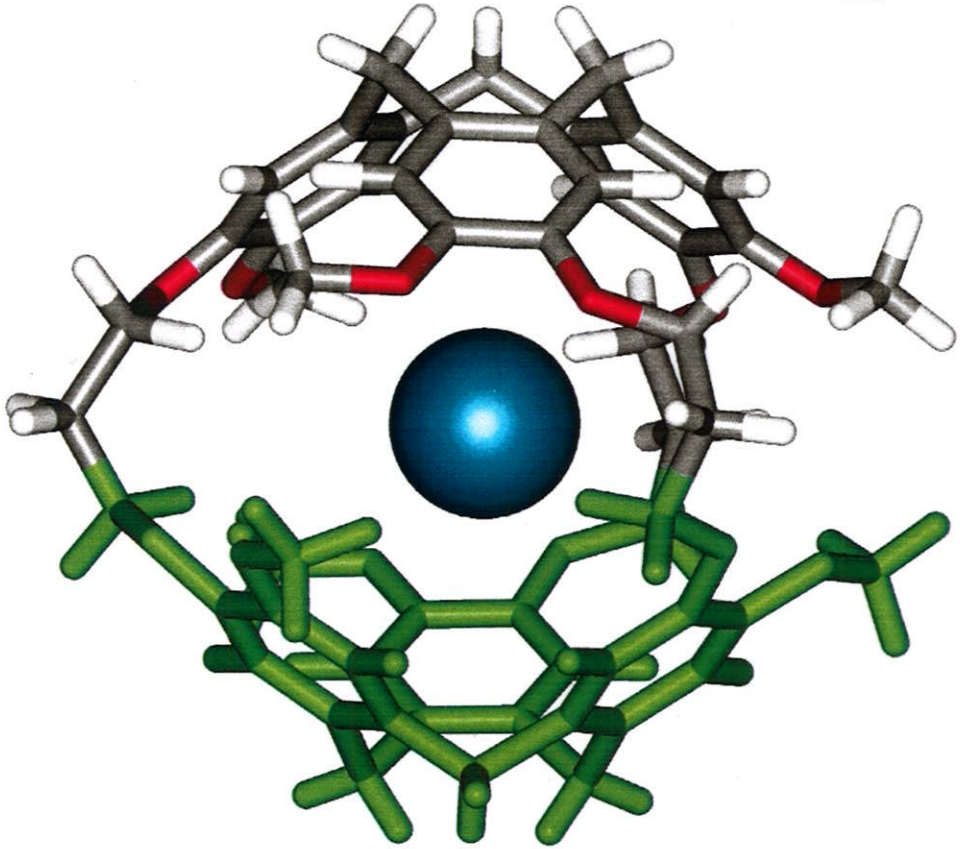

Xe@cryptoE

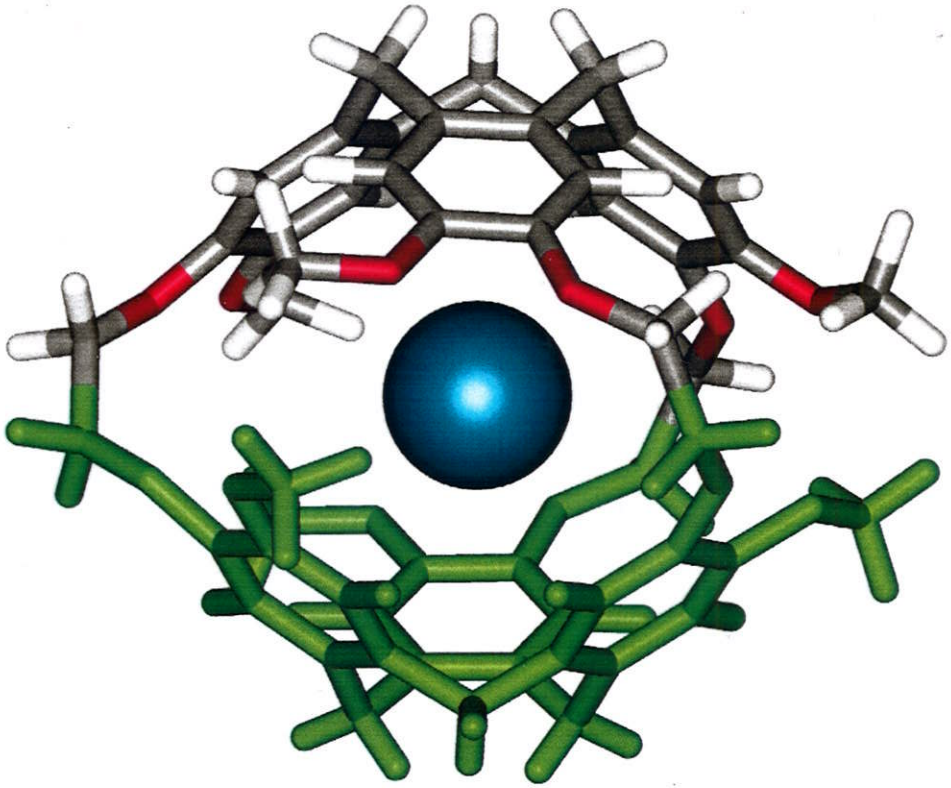

Xe@cryptoA

- Average structure of Xe@cryptoE arrived at using same method
- The same shielding surface can be used for both cages

Xe@cryptoA vs. Xe@cryptoE

Experiment (Pines et al. 2000)*

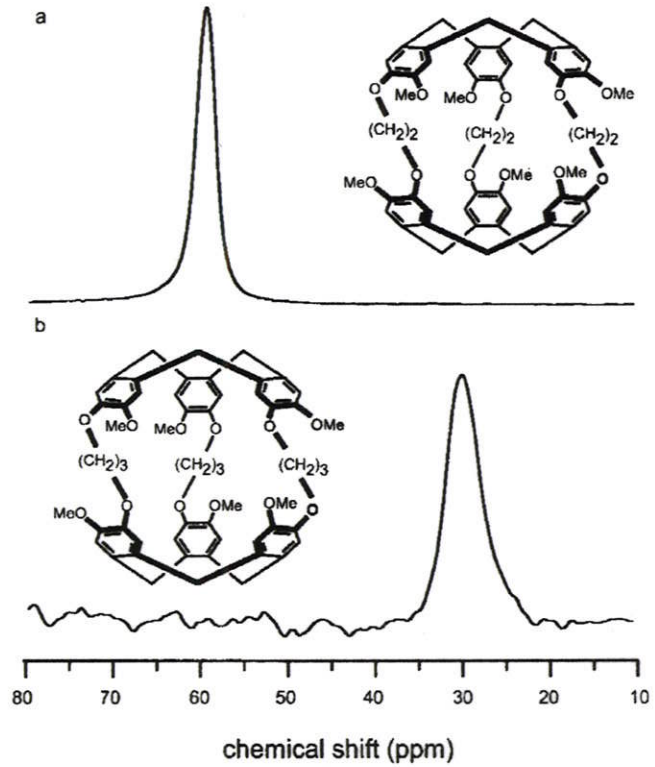

Our MC Simulations

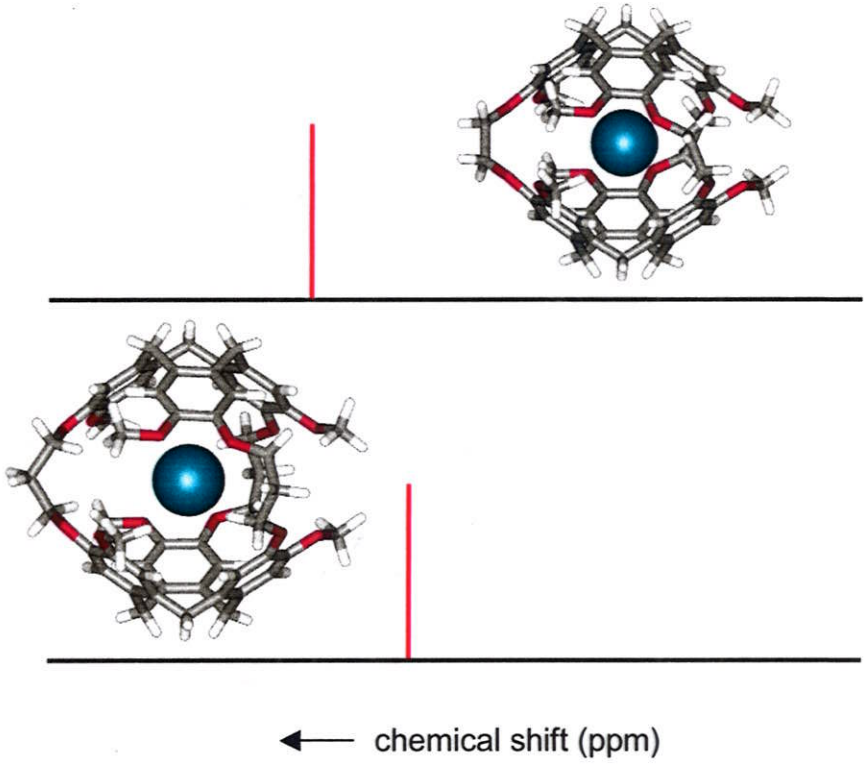

*M.M. Spence, S.M. Rubin, I.E. Dimitrov, E.J. Ruiz, D.E. Wemmer, A. Pines, S.Q. Yao, F. Tian, and P.G. Schultz Proc. Nat. Acad. Sci. **2001**, 98, 10654-10657.

Xe@d_n-cryptoA

Experiment (Brotin et al. 2000)*

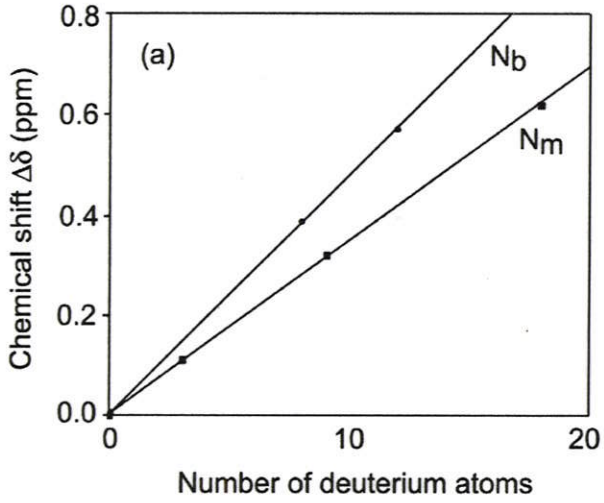

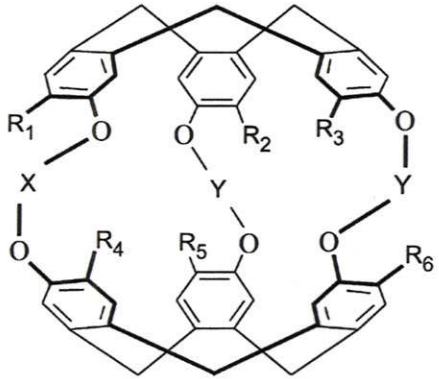

1: X = CH_2CH_2; Y = CH_2CH_2; $R_1 = OCH_3$; $R_2 - R_6 = OCH_3$
2: X = CH_2CH_2; Y = CD_2CD_2; $R_1 = OCH_3$; $R_2 - R_6 = OCH_3$
3: X = CD_2CD_2; Y = CD_2CD_2; $R_1 = OCH_3$; $R_2 - R_6 = OCH_3$
4: X = CD_2CD_2; Y = CD_2CD_2; $R_1 = OCD_3$; $R_2 - R_6 = OCH_3$
5: X = CD_2CD_2; Y = CD_2CD_2; $R_1 - R_3 = OCD_3$; $R_4 - R_6 = OCH_3$
6: X = CD_2CD_2; Y = CD_2CD_2; $R_1 - R_6 = OCD_3$

*T. Brotin, A. Lesage, L. Emsley, and A. Collet, J. Am. Chem. Soc. **2000**, 122, 1171-1174

Our MC Simulations

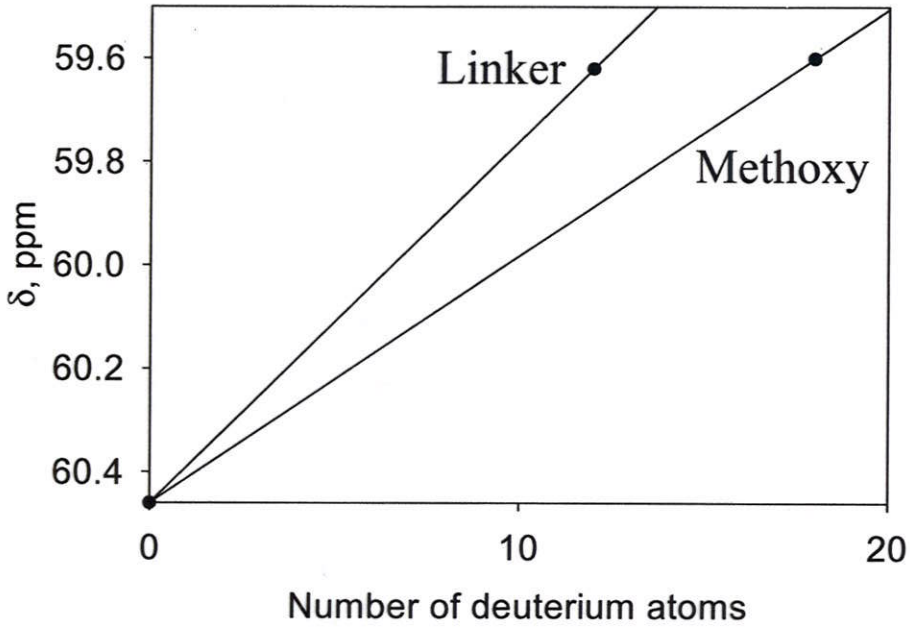

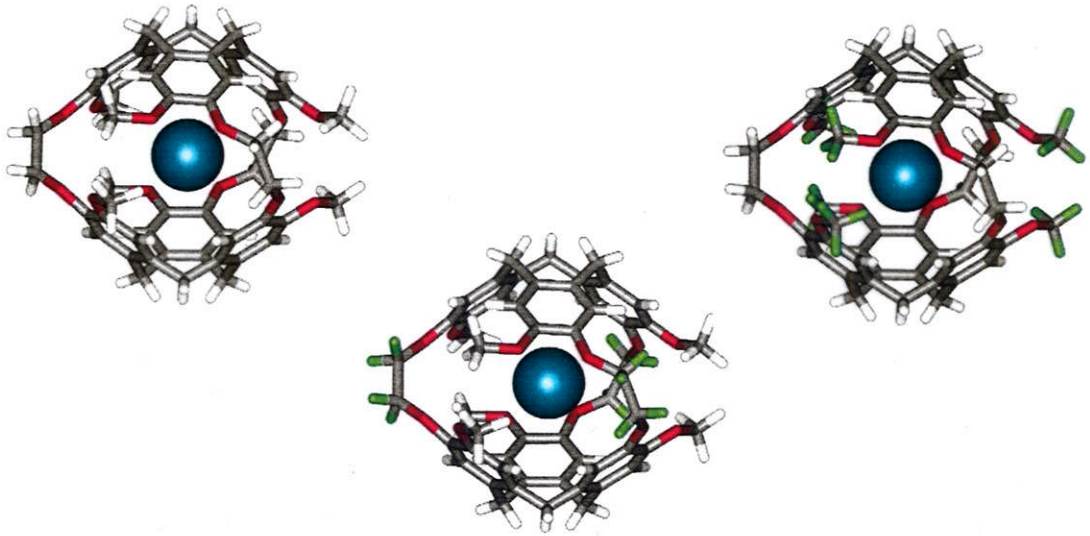

Chemical shifts in chiral environments

Model Systems 1-turn+1

Xe in a left handed helix (L)

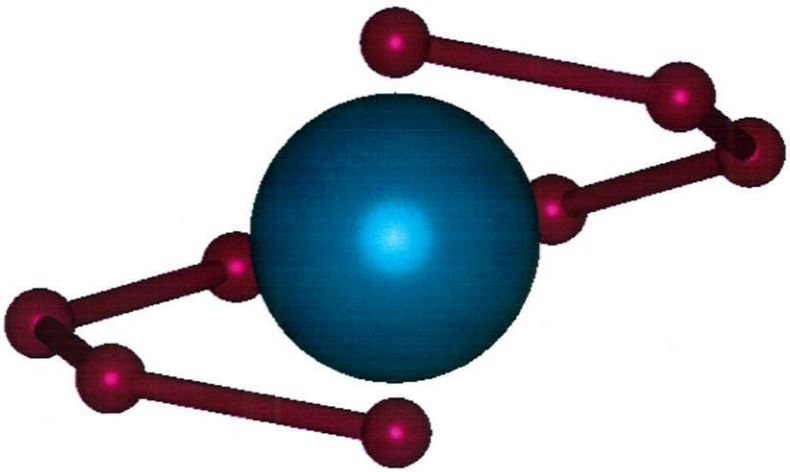

Xe in a right handed helix (R)

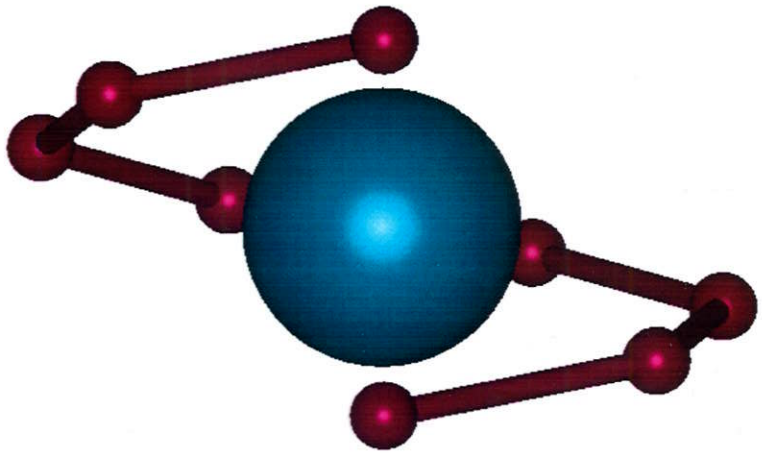

Model Systems 1-turn+1

(L) in a Left handed PCA (Ll)

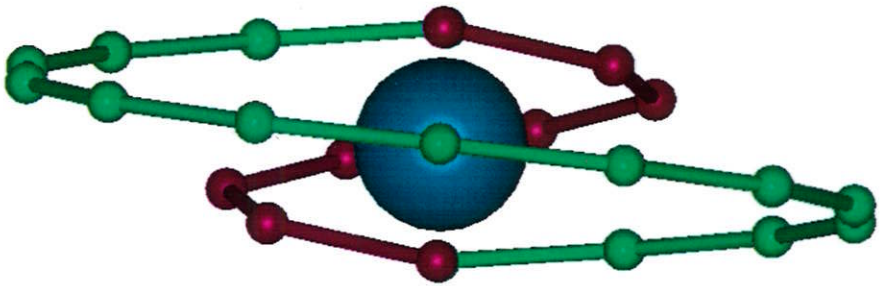

(R) in a right handed PCA (Rr)

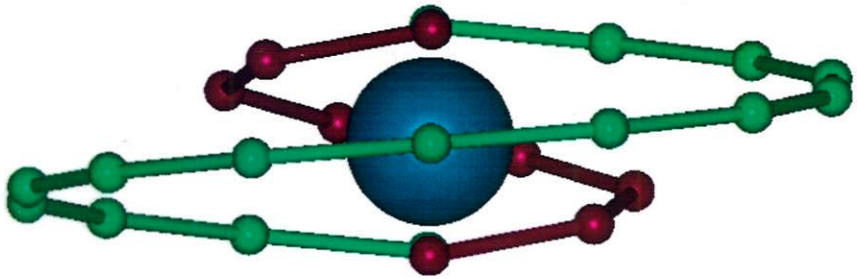

(L) in a right handed PCA (Lr)

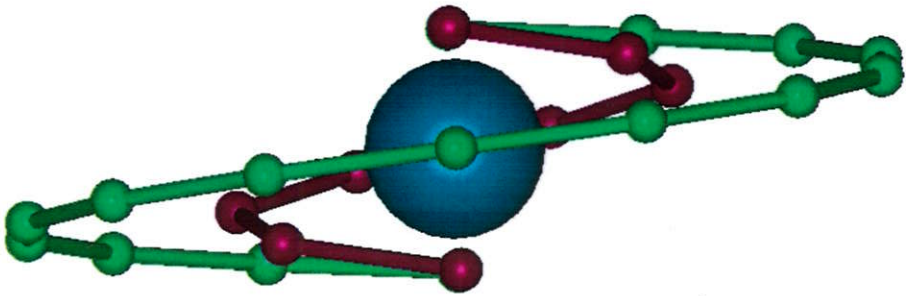

(R) in a left handed PCA (Rl)

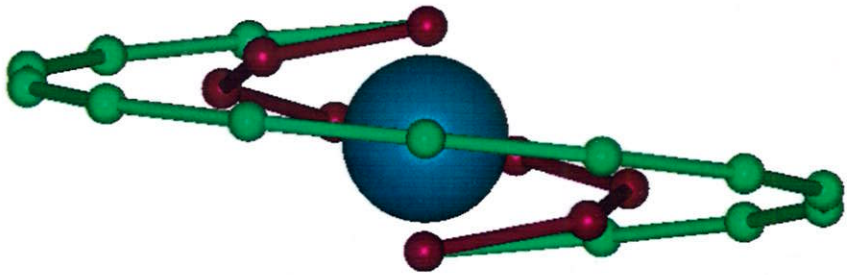

Results 1-turn+1

Model	σ_{iso} (ppm)*
L	-68.9434
R	-68.9434
Ll	-20.9015
Rr	-20.9015
Lr	-19.9673
Rl	-19.9673
Ll-Lr	-0.9342
Rr-Rl	-0.9342

*Relative to the counterpoise corrected free Xe atom at 5642.8466 ppm

Results 1-turn+1
Neutron Calc.

Model	σ_{iso} (ppm)
L	-0.0016
R	-0.0016
Ll	0.9218
Rr	0.9218
Lr	0.9409
Rl	0.9409
Ll-Lr	-0.0191
Rr-Rl	-0.0191

1-turn+1 model

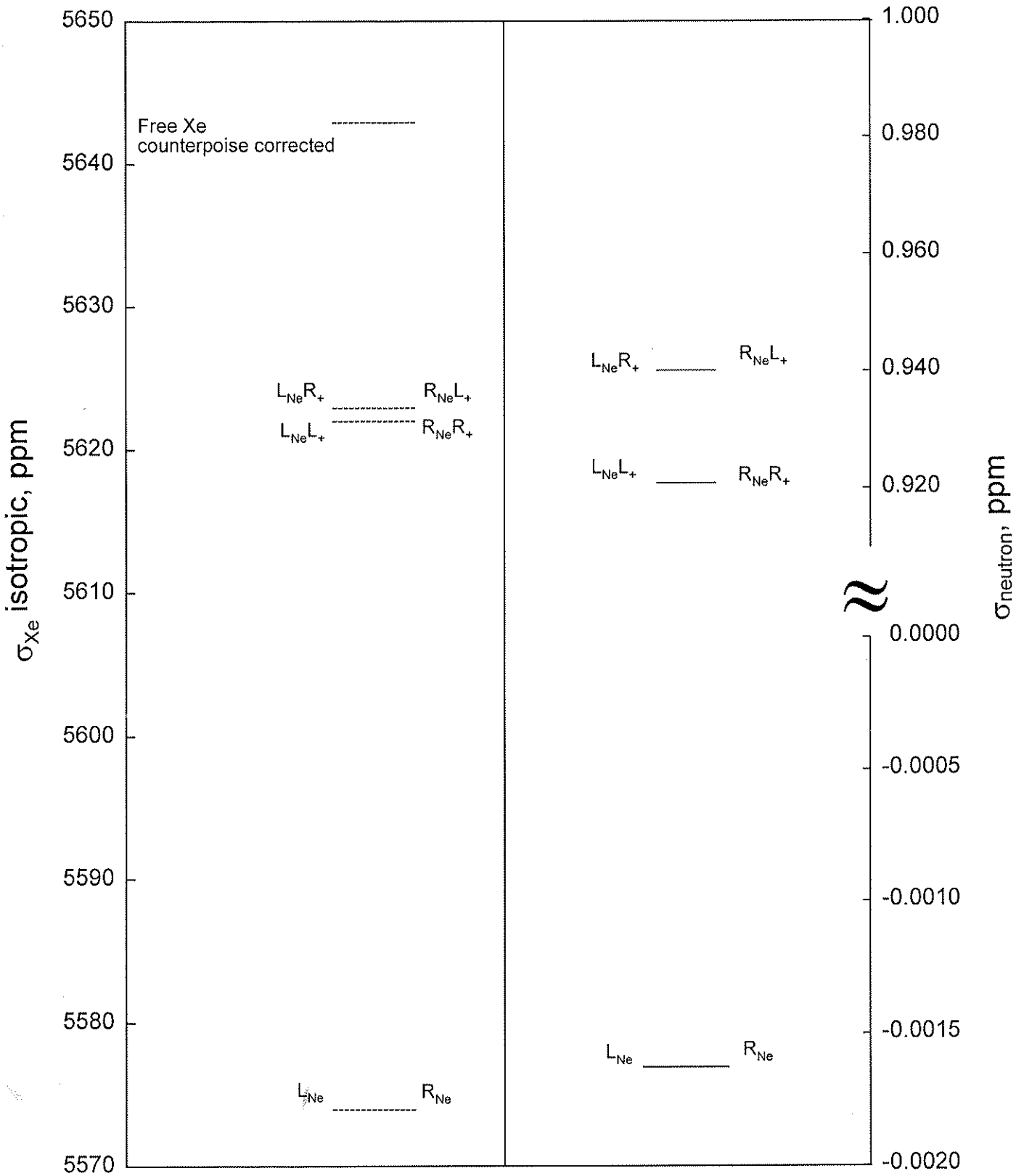

“Electrostatic contributions” to chemical shifts

hydrogen-bonded environments

MOTIVATION

- Xe chemical shieldings and quadrupolar coupling interactions are very sensitive to void size and shape in clathrates[1,2]
- Structure of Xe clathrate hydrates of type I:

  Cubic unit cell: a = 11.9825 Å, 46 water molecules

  2 types of cages: 5^{12} ("small") : $5^{12}6^2$ ("large") = 1: 3

  3-D disordered hydrogen-bonded network of H_2O molecules

5^{12} Cage - $(H_2O)_{20}$

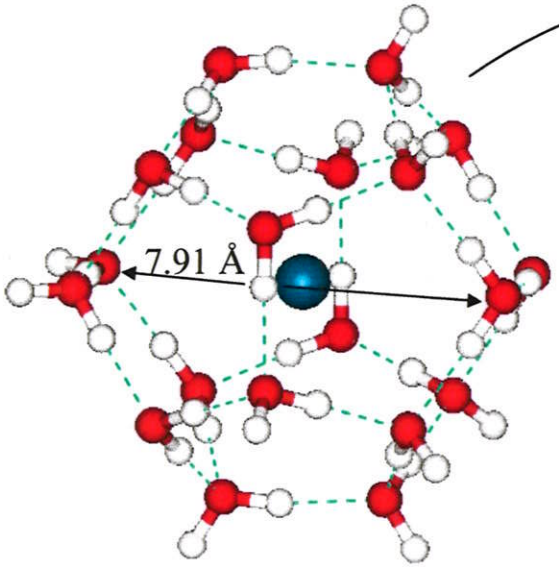

Dodecahedron of 12 pentagonal faces

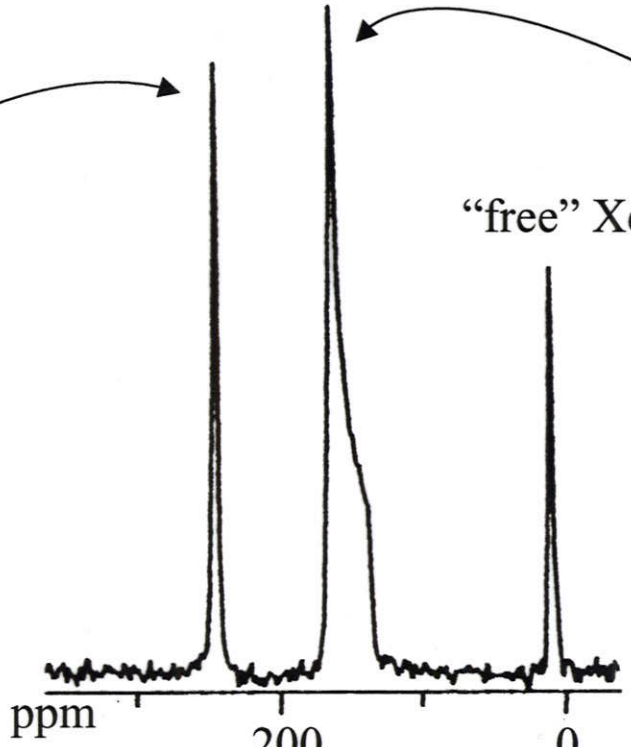

Moudrakovski et al.[2]

$5^{12}6^2$ Cage - $(H_2O)_{24}$

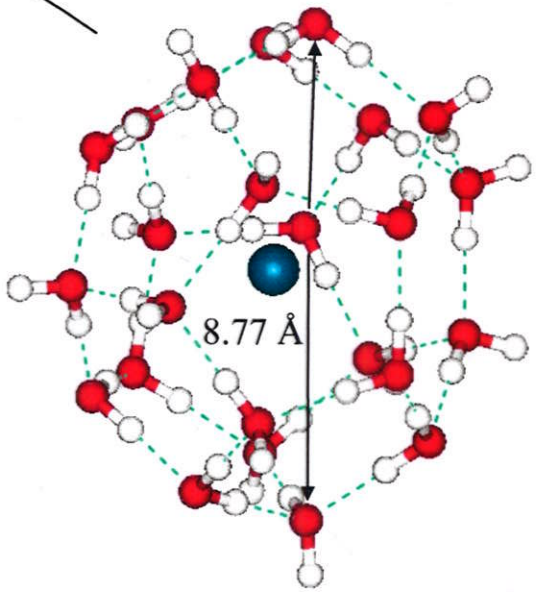

14-hedra of 12 pentagonal and two hexagonal faces

- H_2O molecules are represented either by point charges or quantum mechanically at HF/D95** and B3LYP/D95** levels of theory
- Xe is represented with 240 basis functions

MODELS

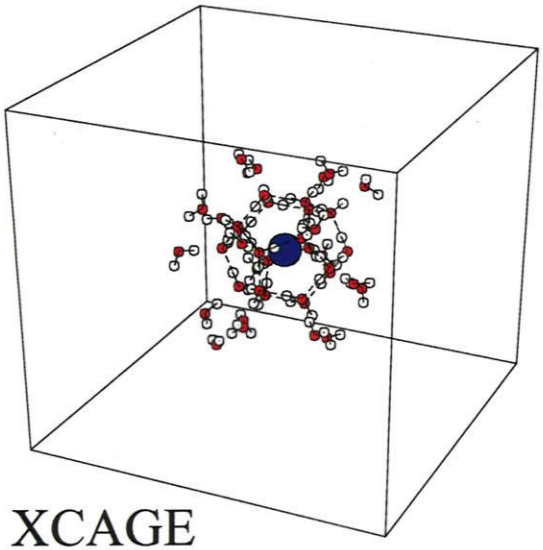

XCAGE

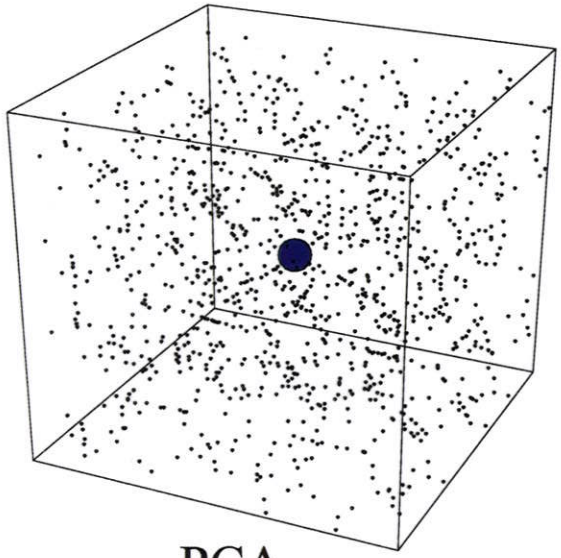

PCA

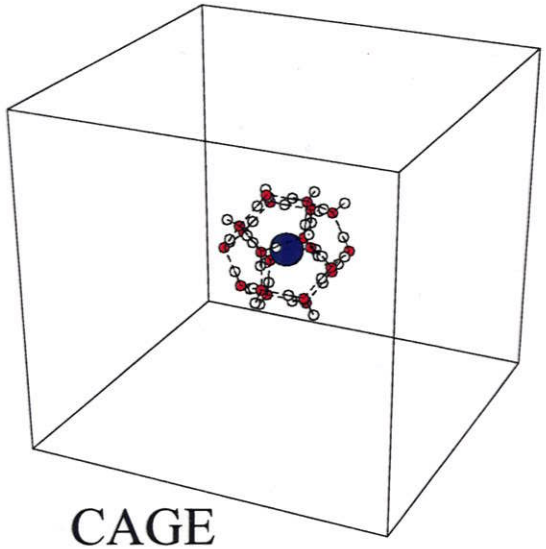

CAGE

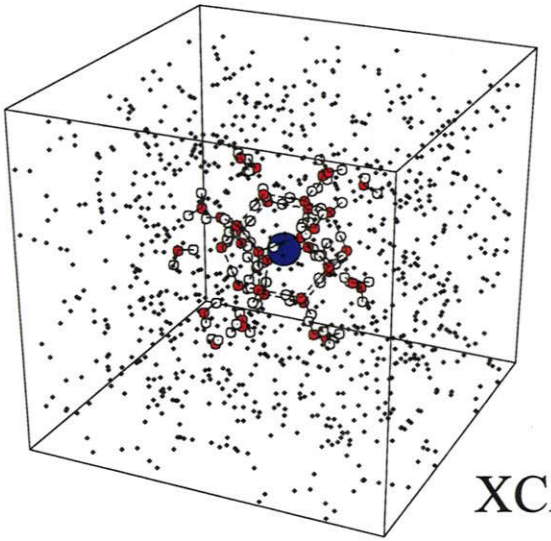

XCAGE/PCA

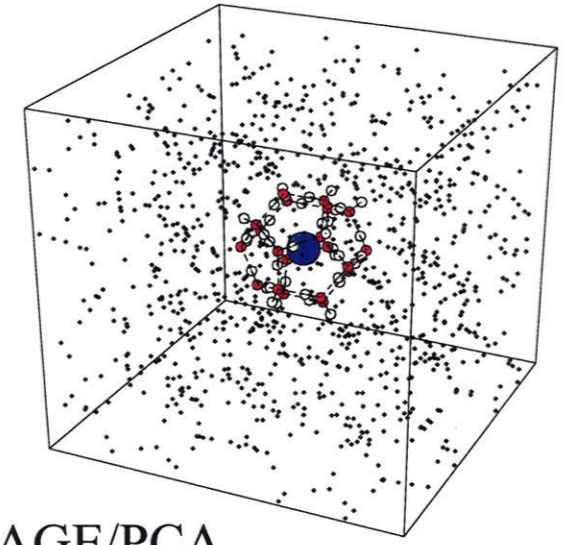

CAGE/PCA

Xe AB INITIO ISOTROPIC SHIELDINGS

Single point shielding, Xe at center of cage, proton configuration 1

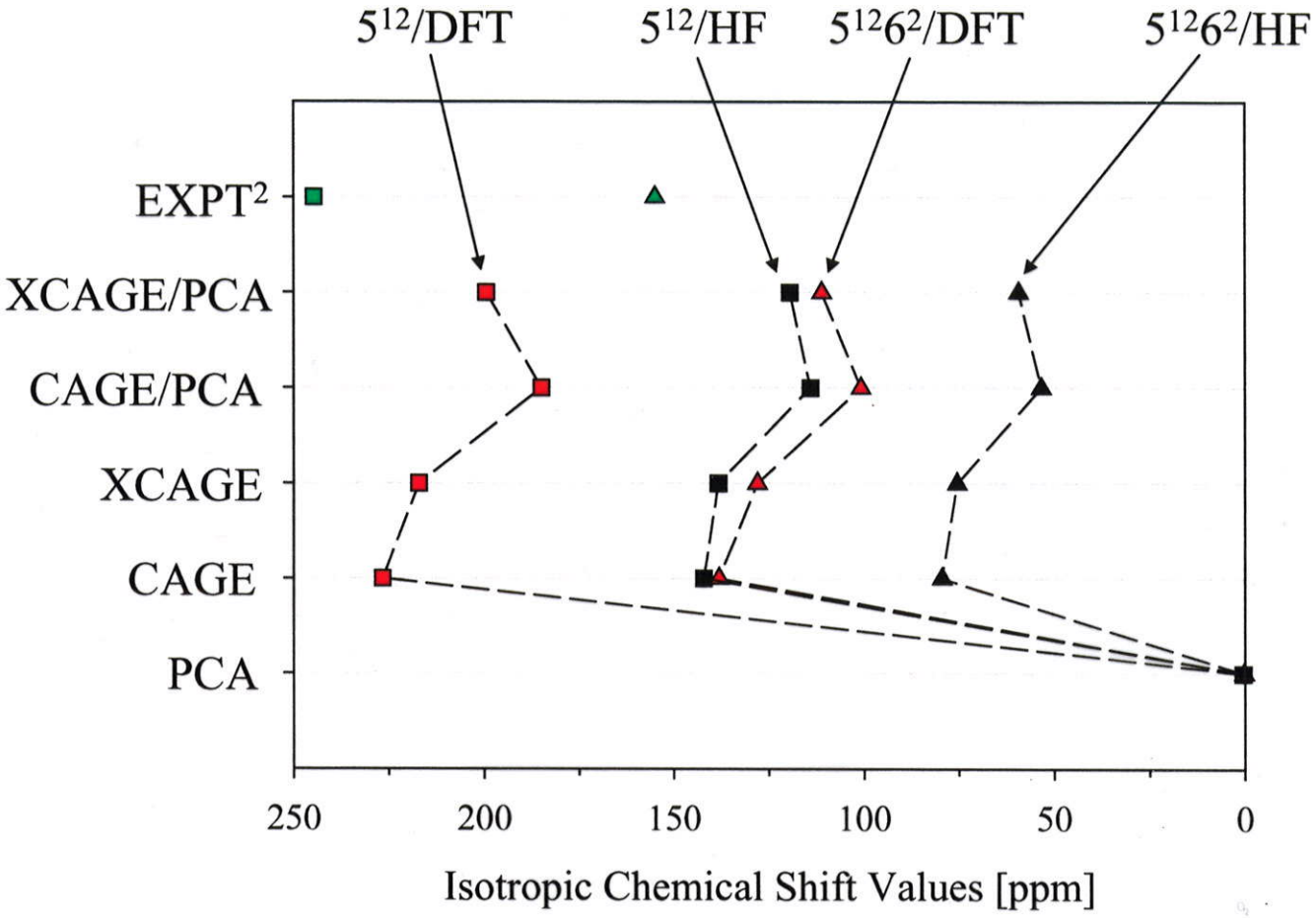

Findings:

- Electron correlation has to be included in QM calculations
- PCA model produces insignificant shielding response
- CAGE (not hydrogen-bonded to other H_2O molecules) → highest shielding response
- Use of point charge array to account for hydrogen-bonding of cage to crystal gives incomplete response
- For realistic response, need "real" H_2O molecules hydrogen-bonded to cage and point charge array, e.g., XCAGE/PCA model

THE Xe SHIELDING SURFACES

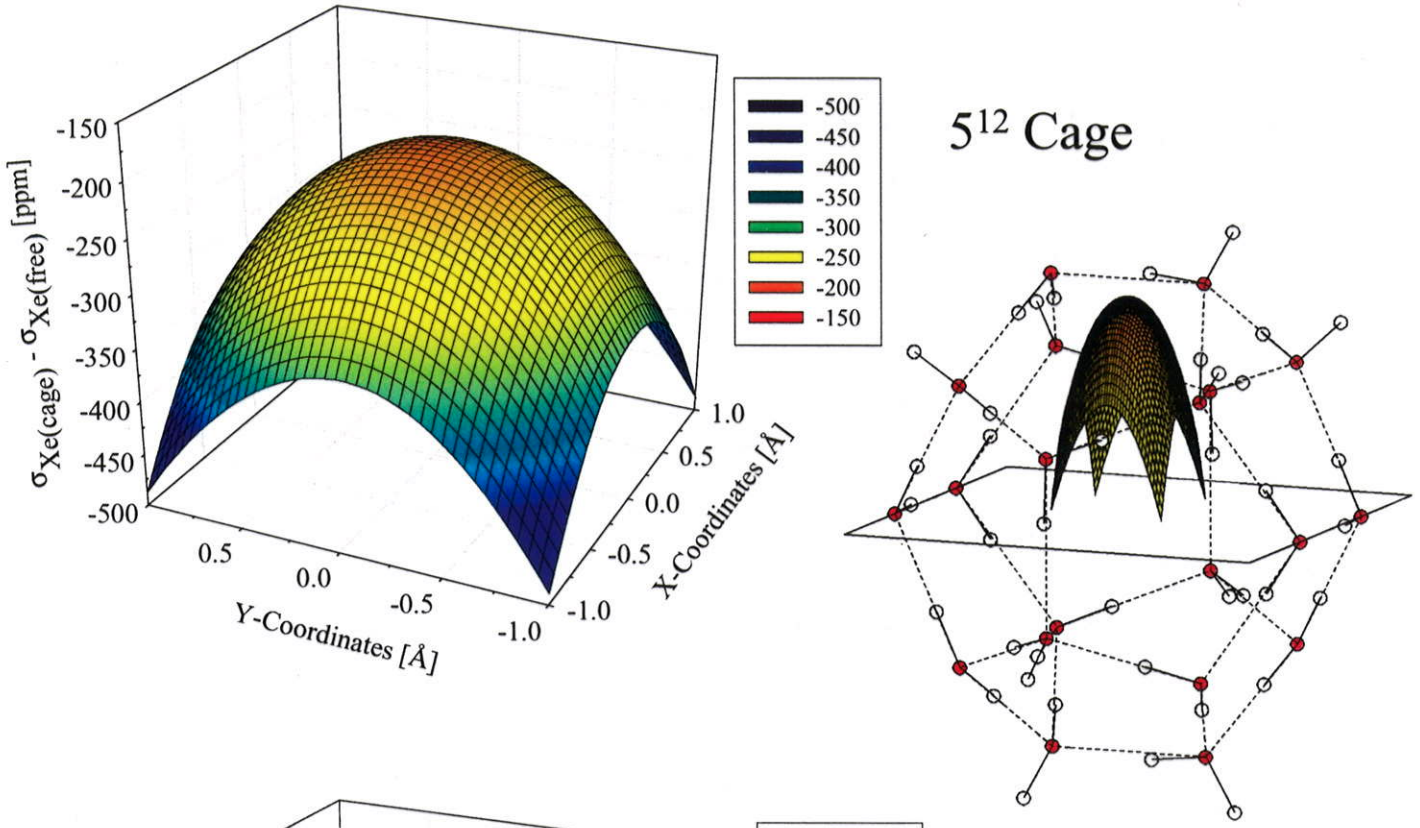

5^{12} Cage

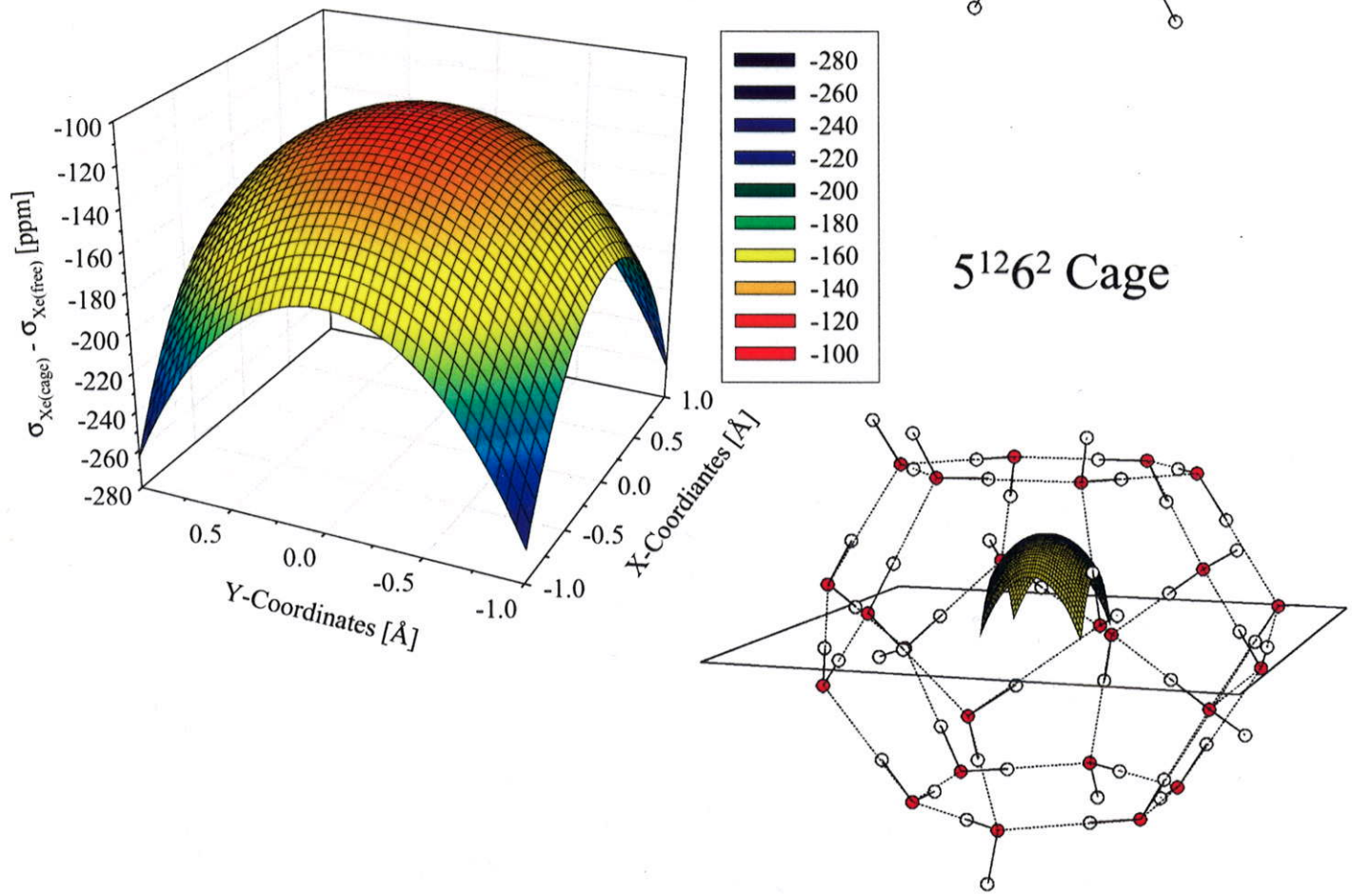

$5^{12}6^{2}$ Cage

METROPOLIS MONTE CARLO SHIELDING AVERAGING

Use ab initio shielding surface and Lennard-Jones V(Xe-O)[5]:

$r_0 = 3.700$ and $\varepsilon = 0.753$ kJ/mol

Results:

- Xe one-body distribution functions at 275 K:

5^{12} Cage

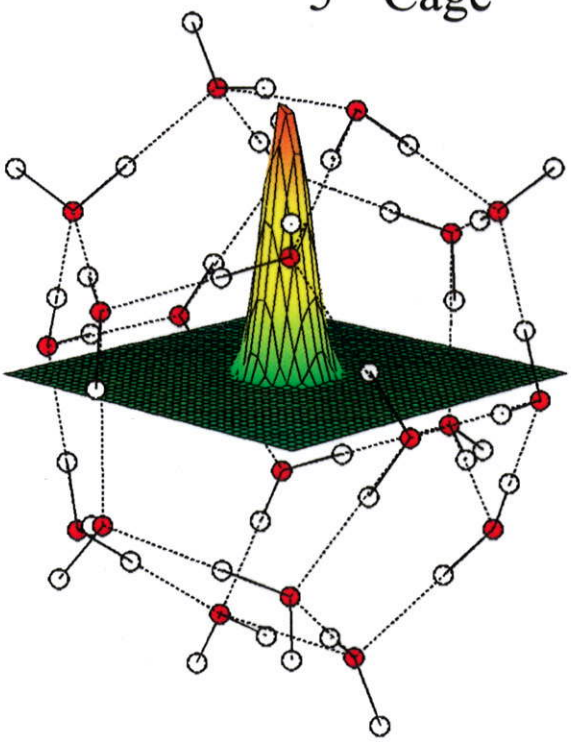

$5^{12}6^2$ Cage

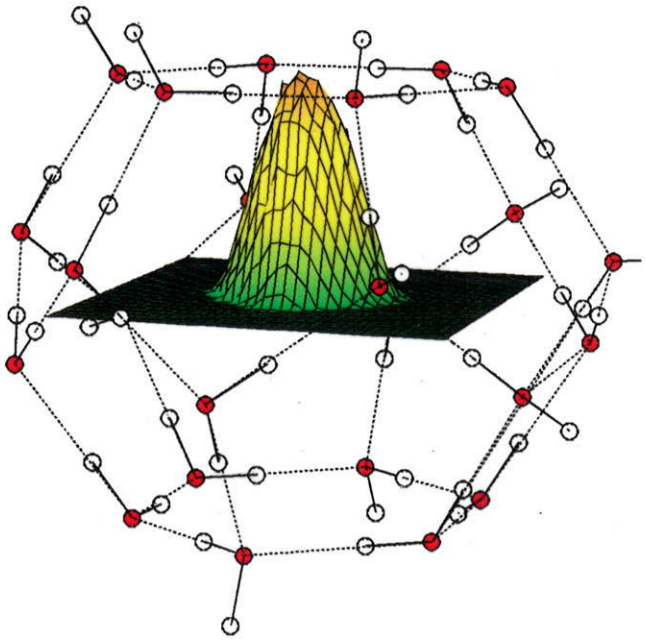

- Xe atom moves within a sphere of approximately R = 1 Å
- Xe isotropic chemical shift values, ppm

Method	Small Cage	Large Cage
EXPT[2]	244.6	154.9
XCAGE/PCA	225.3	143.8

CONCLUSIONS

- The NMR chemical shift is exquisitely sensitive to the environment in which the nucleus finds itself.
- Encoded in the intrinsic shielding response surface is the electronic structure of the molecule or the supermolecule as a function of nuclear configuration.
- The dynamic averaging encodes further information about the nuclear environment into the observed chemical shift.
- There are many applications to problems of immediate interest to chemists, biochemists and material scientists that take advantage of the site-specific nature of this property.

Acknowledgments:

with *Devin N. Sears*:
Xe in Xe-Rg
Xe in cryptophane cage
chiral shielding
Xe in TPP channel
Xe@C_{60}

with *Dirk Stueber*:
Xe in clathrate hydrate Structure I